

From UV to Near-Infrared light detection: next generation photodetectors for imaging and biometric applications

Dr Nicola Gasparini

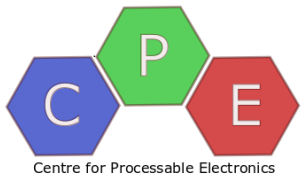
Department of Chemistry Imperial College London
Centre of Processable Electronics

n.gasparini@imperial.ac.uk

𝕏 @nicogaspa

Sino-Germany Workshop, Erlangen, May 21st, 2024

IMPERIAL



The Gasparini group

Polina Jacoutot

Francesco Furlan

Tianyi Zhang

Zhuoran Qiao

Davide Nodari

Prof. Martin Heeney

Dr Julianna Panidi

Prof. James Durrant

Prof. Martyn McLachlan

Dr Artem Bakulin

Prof. Ji-Seon Kim

FAU

Prof. Christoph Brabec



Prof. Iain McCulloch



Prof. Derya Baran

Prof. Thomas Anthopoulos

Dr Alberto Scaccabarozzi

Prof. Sahika Inal



POLITECNICO
MILANO 1863

Prof. Giulio Cerullo

Dr Franco Camargo

TU Delft

Prof. Achilleas Savva



Imperial College London

Dr Christos Chochos



Dr Armin Ardalan



Dr Oskar Sandberg

Funding



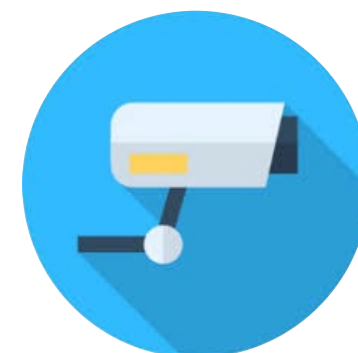
Engineering and
Physical Sciences
Research Council



Internet of Things



Photovoltaics



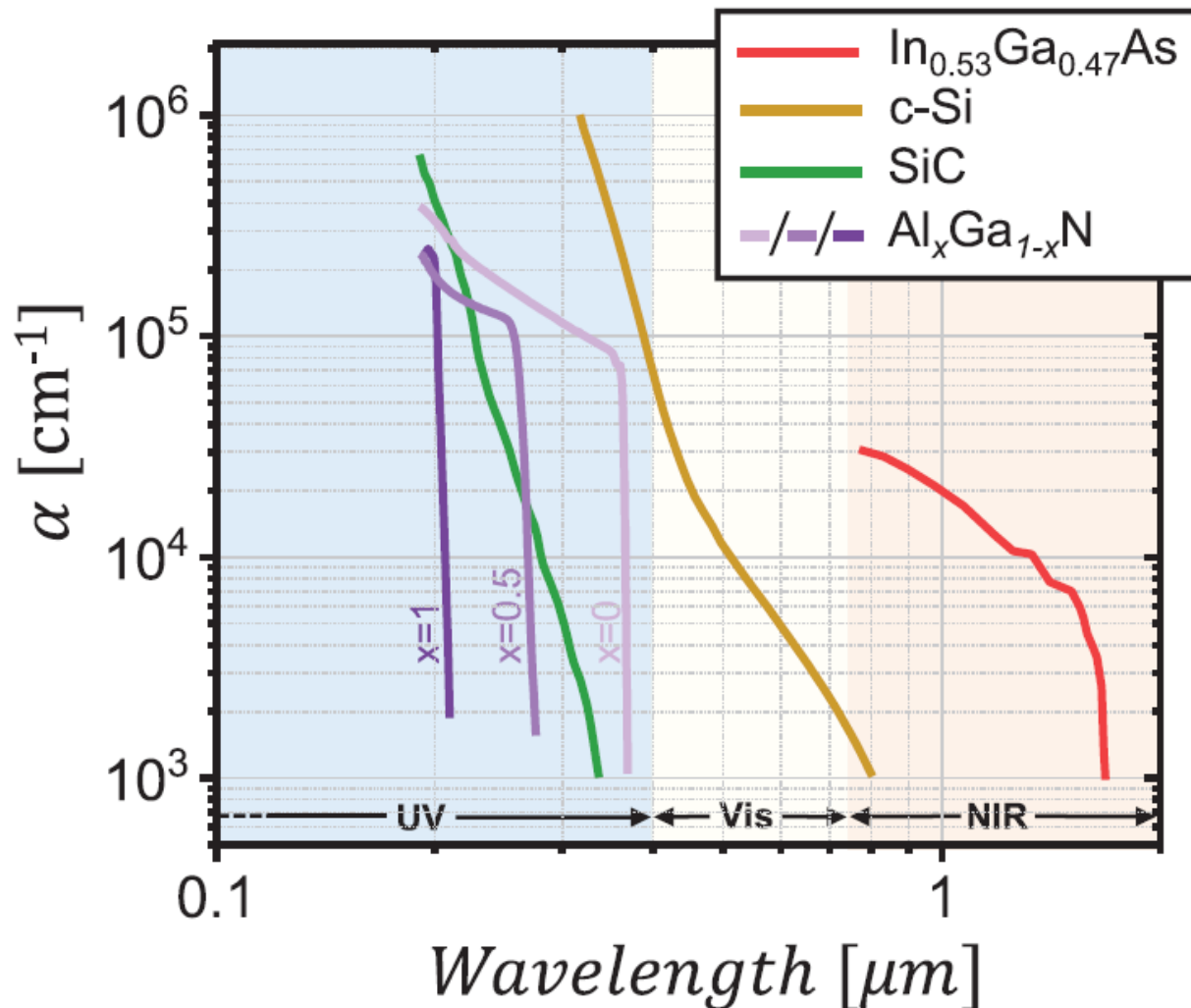
Photodetectors



Healthcare sensors

Industrial IoT market size worldwide for 2025 predicted to be \$111 billion!

State-of-the-art Inorganic PD Technologies



UV: CsI and Cs_2Te broadband photomultiplier tubes (PMTs) → bulky and fragile

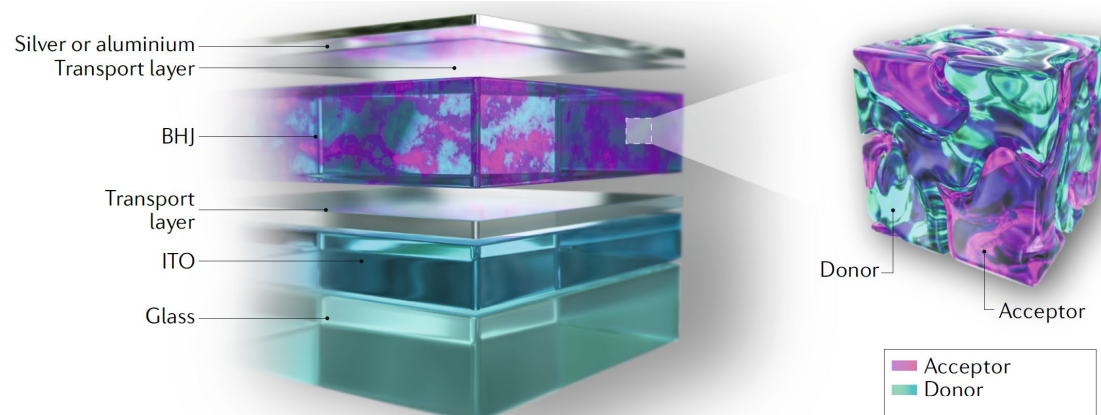
Vis: c-SI and III-V semiconductors requires optical filtering for narrowband → fabrication complexity, high T processes

NIR: InGaAs broadband, input filtering through bulky diffraction gratings or interferometers → £££

Organic photovoltaics vs organic photodetectors

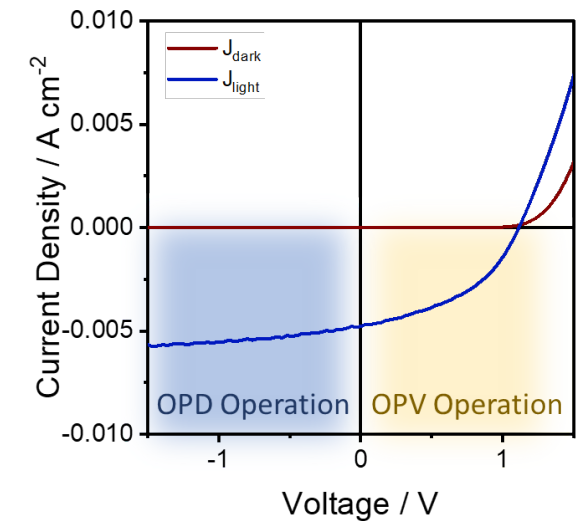
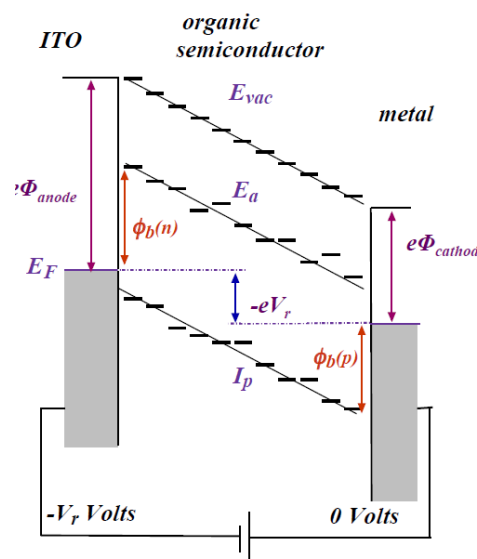
Similarities

- Diode Architecture
- Necessity to extract current generated from light



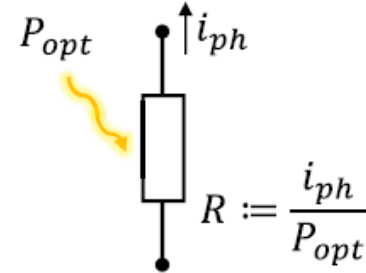
Key Differences

- For Photovoltaics we maximise power output whereas for Photodetectors we want to simultaneously optimise responsivity, detectivity and speed of response
- Photovoltaics are operated at forward bias whereas photodetectors are operated at reverse bias

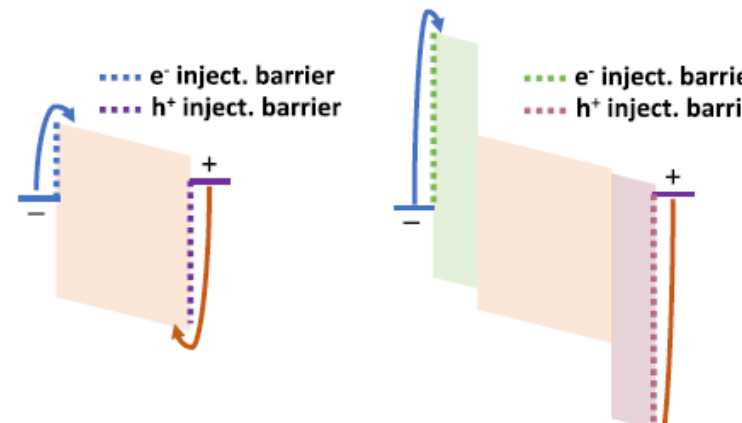


Figures of Merits

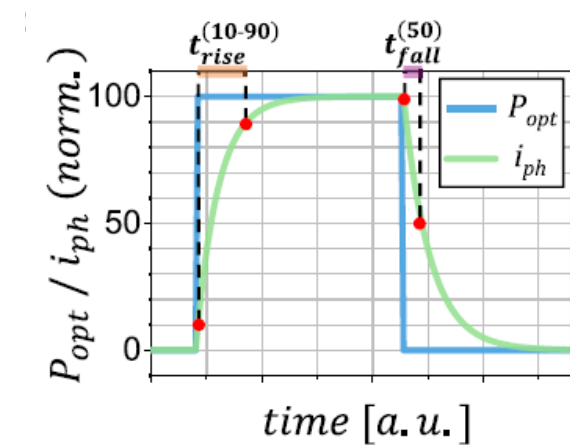
RESPONSIVITY (EQE)



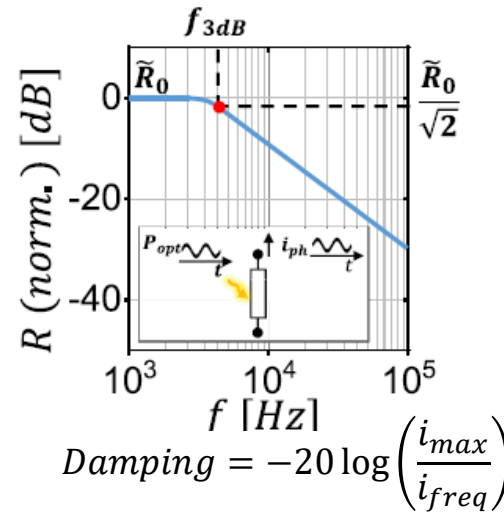
DARK CURRENT (Jd)



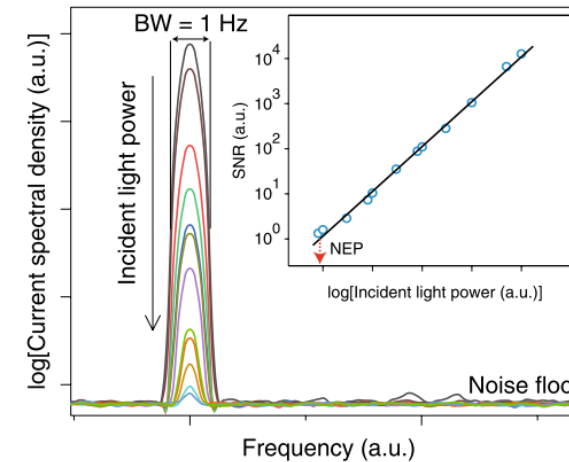
RISE/FALL TIMES



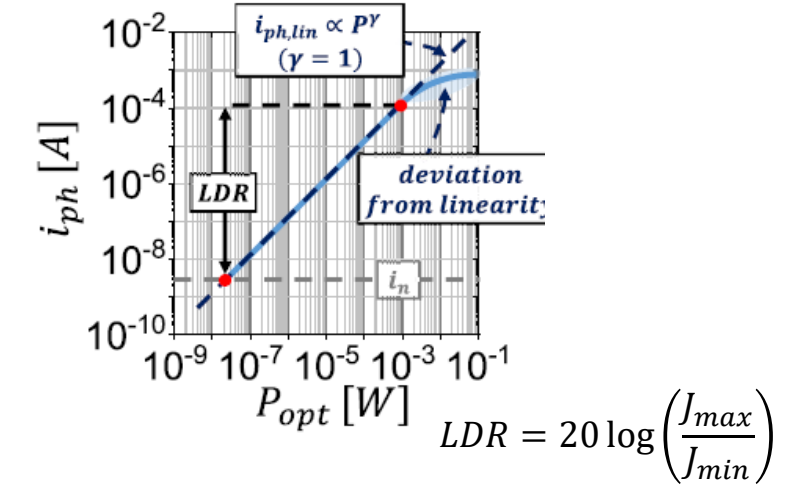
CUT-OFF FREQUENCY



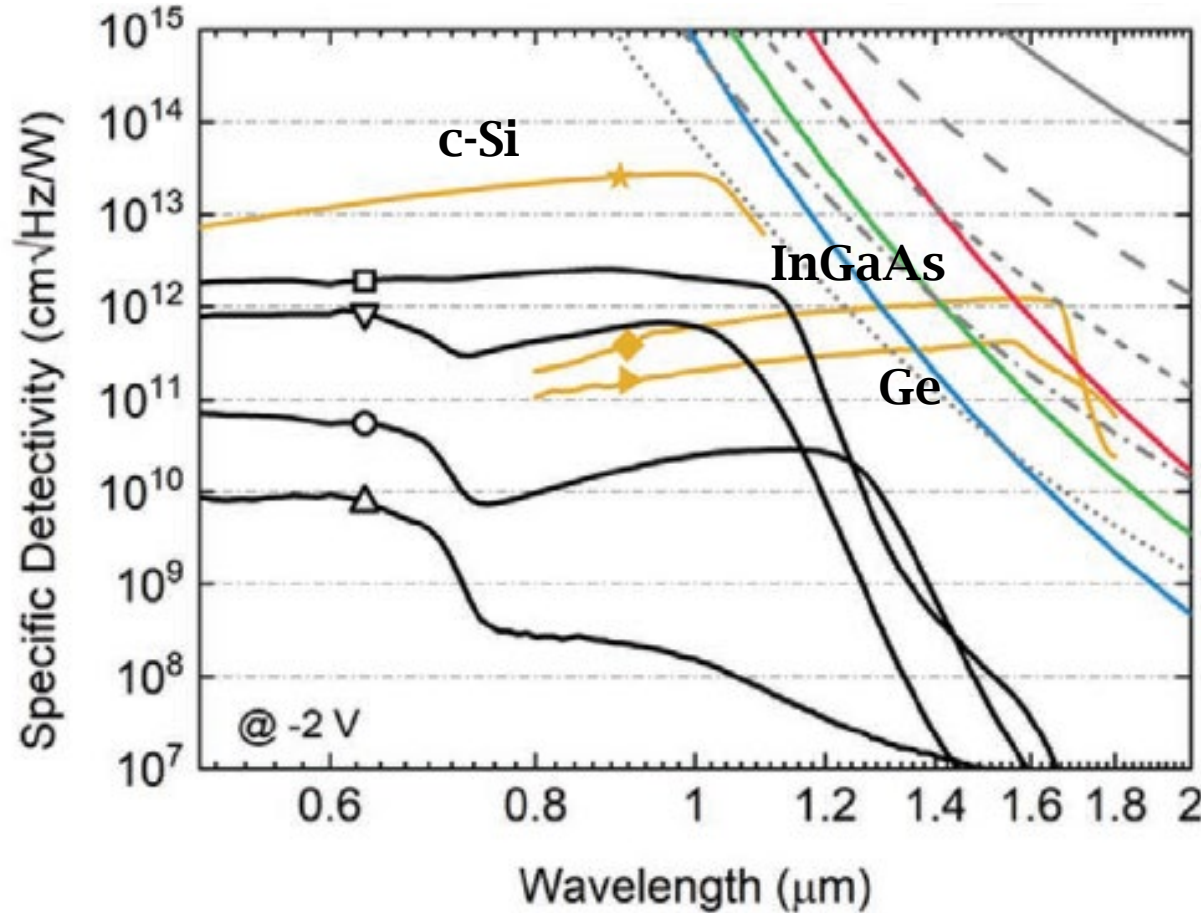
NOISE EQUIVALENT POWER (NEP)



LINEAR DYNAMIC RANGE (LDR)



Specific Detectivity (D^*)



$$D^* = \frac{\sqrt{A\Delta f}}{NEP}$$

The noise describes the statistical fluctuations of the current over time $i(t)$ around an average value i_{mean} . The root mean square value of this fluctuation is called noise current i_{noise}

$$i_{\text{noise}}(f) = \sqrt{i_{\text{shot}}^2 + i_{\text{thermal}}^2 + i_{1/f}^2(f)} \quad [\text{A Hz}^{-1/2}]$$

$$i_{\text{shot}} = \sqrt{2qi_{\text{dark}}} \quad [\text{A Hz}^{-1/2}]$$

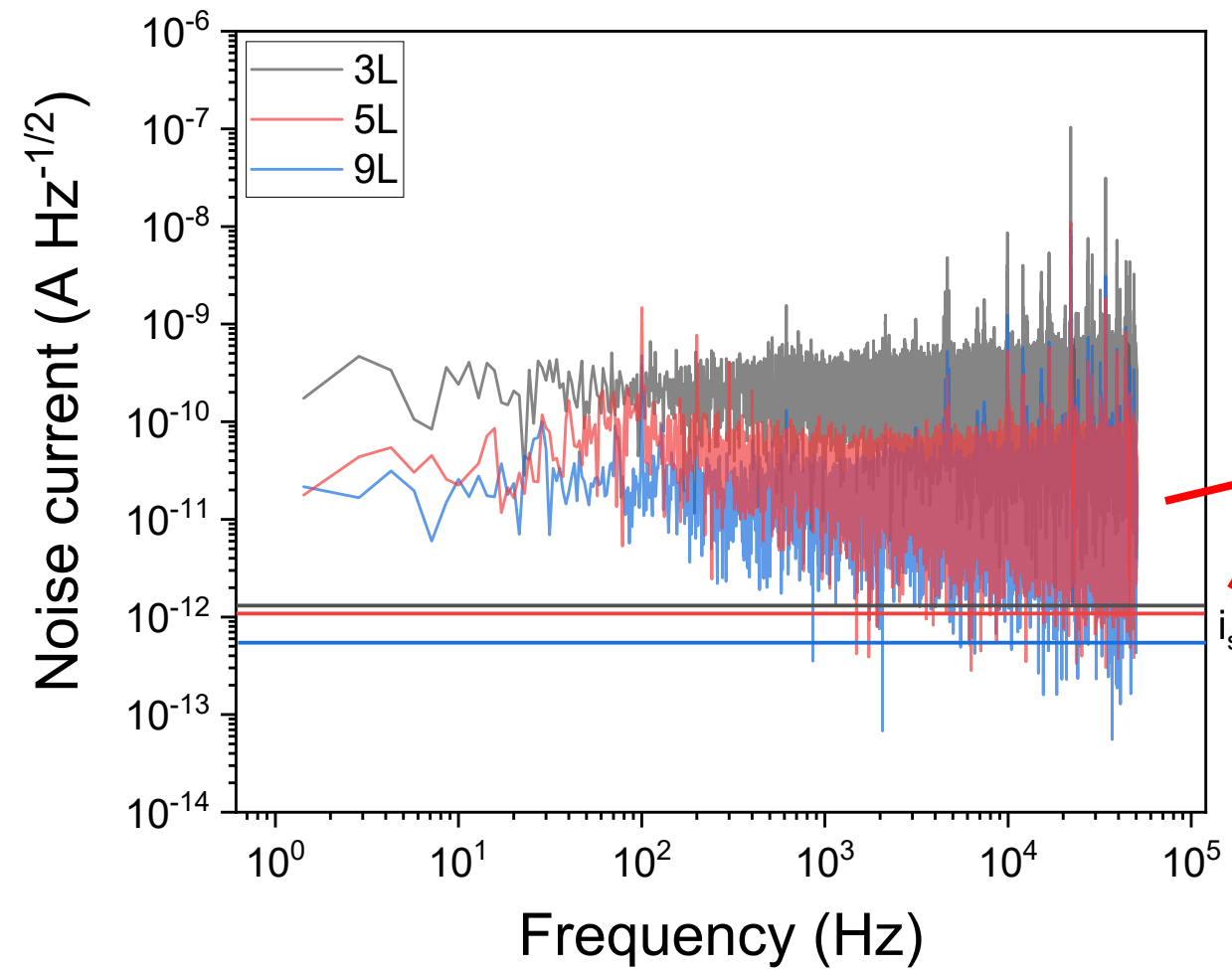
$$i_{\text{thermal}} = \sqrt{4k_B T R_{\text{shunt}}^{-1}} \quad [\text{A Hz}^{-1/2}]$$

$$i_{1/f} \propto \frac{1}{f} \quad [\text{A Hz}^{-1/2}]$$

Shot noise → represents fluctuations in the charge carrier distribution over time and space

Thermal noise → results from thermal excitation of charge carriers

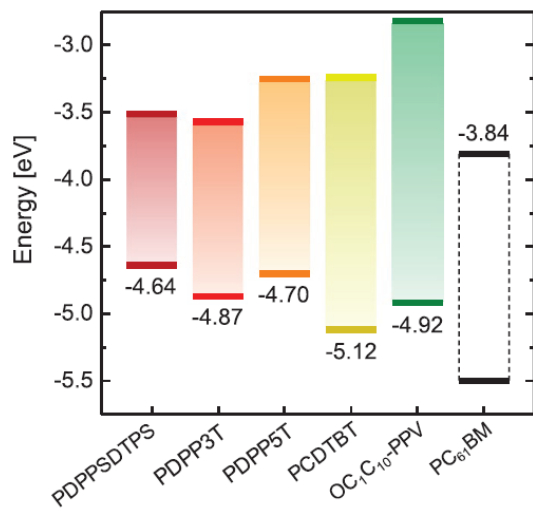
frequency-dependent sources, generation and recombination of electron-hole pairs.



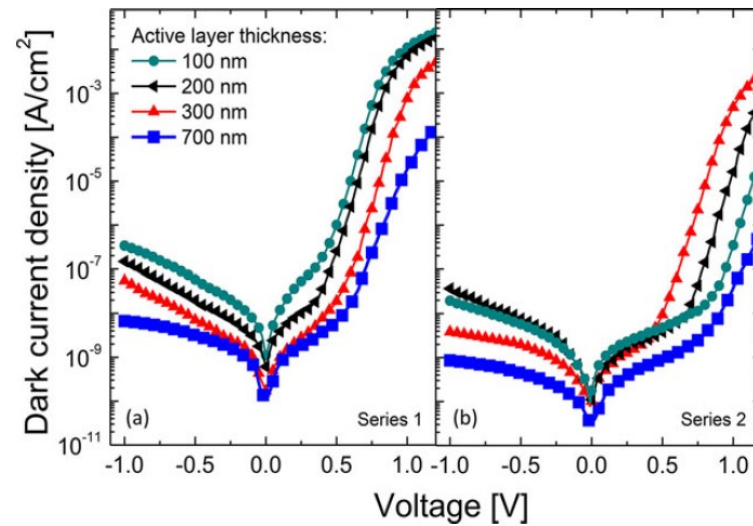
$$i_{noise}(f) = \sqrt{i_{shot}^2 + i_{thermal}^2 + i_{1/f}(f)^2}$$

- This is the **calculated noise**
- The **measured noise** is always higher because takes into account all the sources of the white noise that are not considered in the model

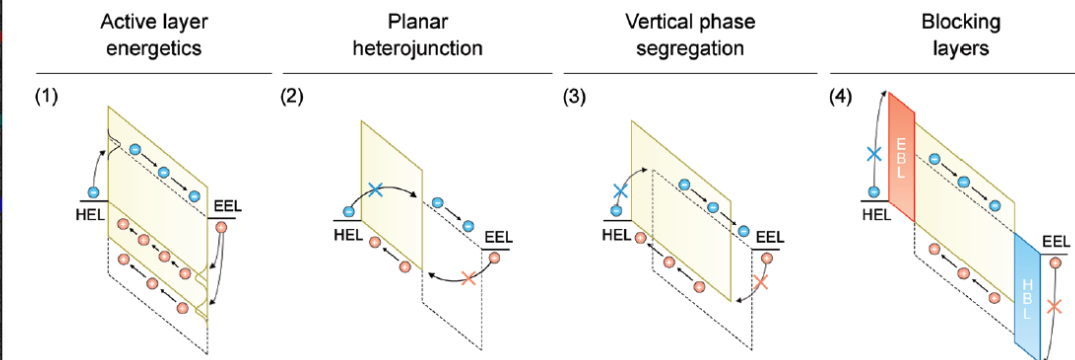
Materials energetics



Active layer thickness



Hole/Electron Blocking Layer



Adv. Optical Mater. 2020, 8, 1901568

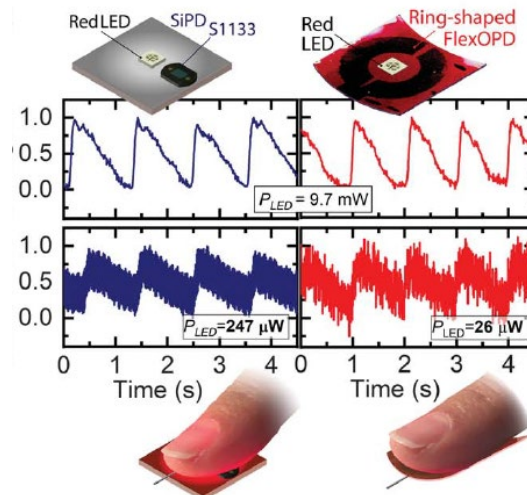
Laser and Photonics Reviews. 2014, 8, 924.

Adv. Funct. Mater. 2020, 30, 1904205

Infrared organic photodiodes

Why Infrared Photodetectors?

- Biological windows (NIR-II: 1000 – 1300 nm) and NIR-III: 1550 – 1870 nm), which offer deeper tissue penetration, improved image contrast and reduced photobleaching
- Night cameras



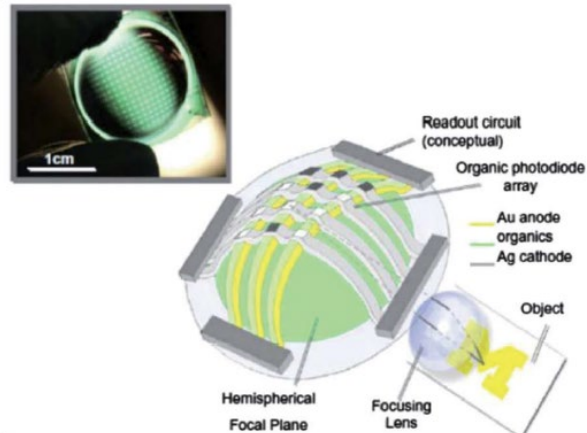
Wang et al. 2020



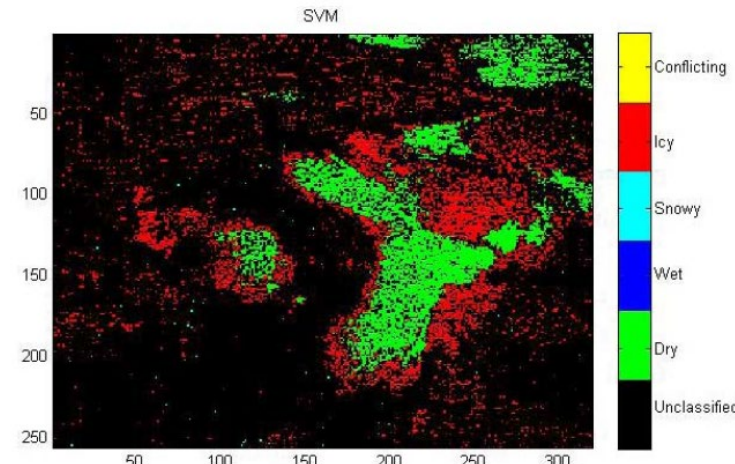
Khan et al. 2020

Why NIR-OPDs?:

- conformal coverage
- biocompatibility
- cooling requirements
- preferred choice for wearable health monitors



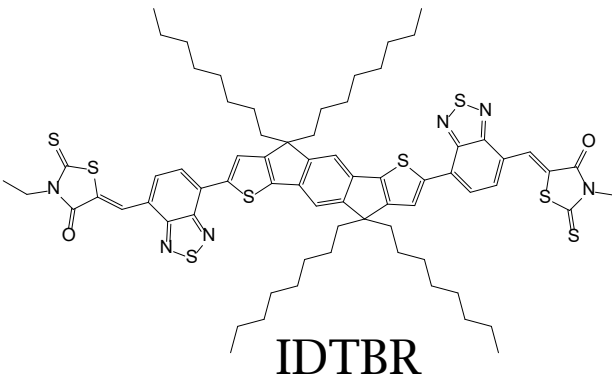
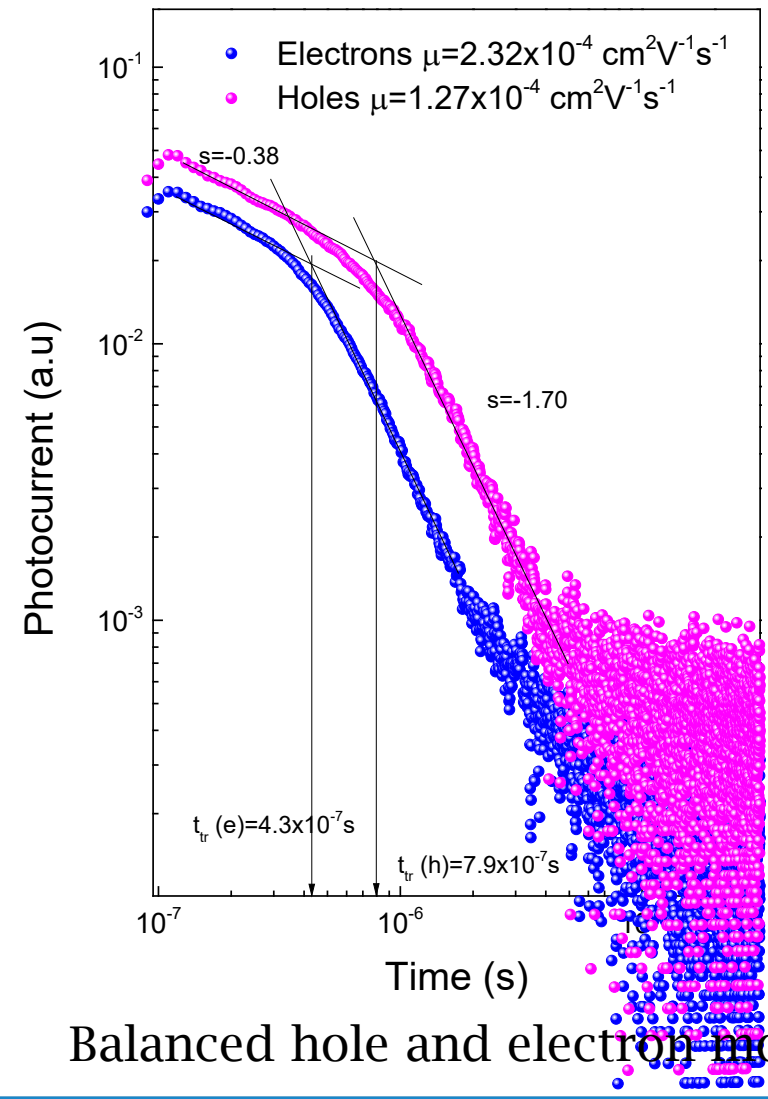
K.-H. Jeong, Science, 2006



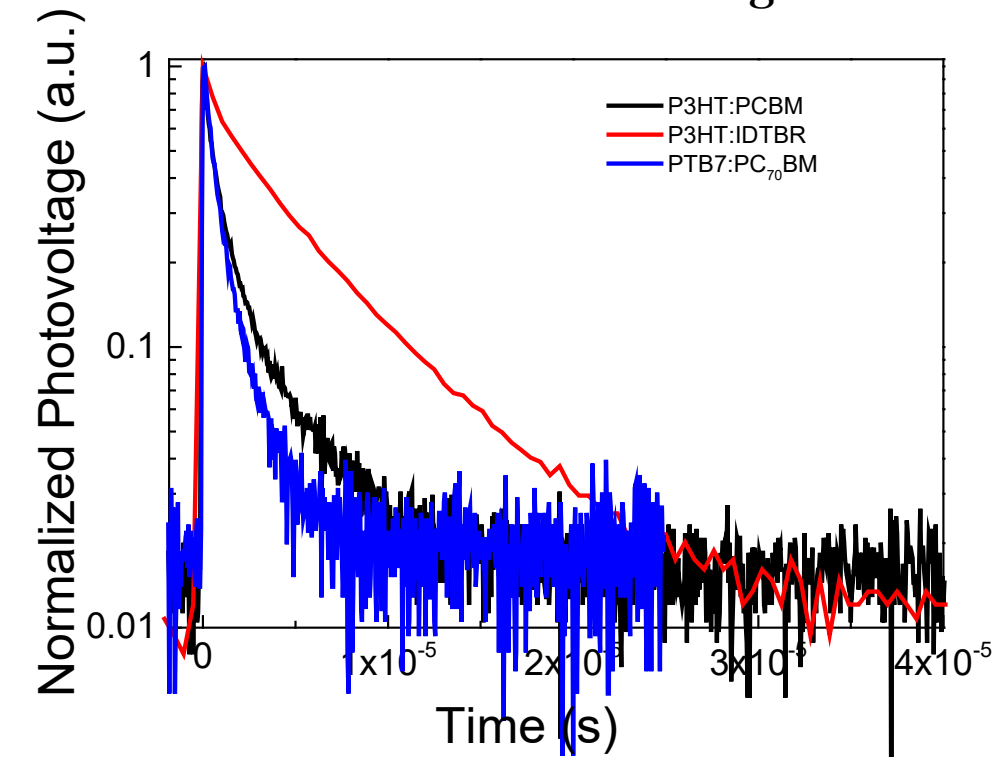
Jonsson et al. 2015

Charge carrier mobility and lifetime

Time of flight

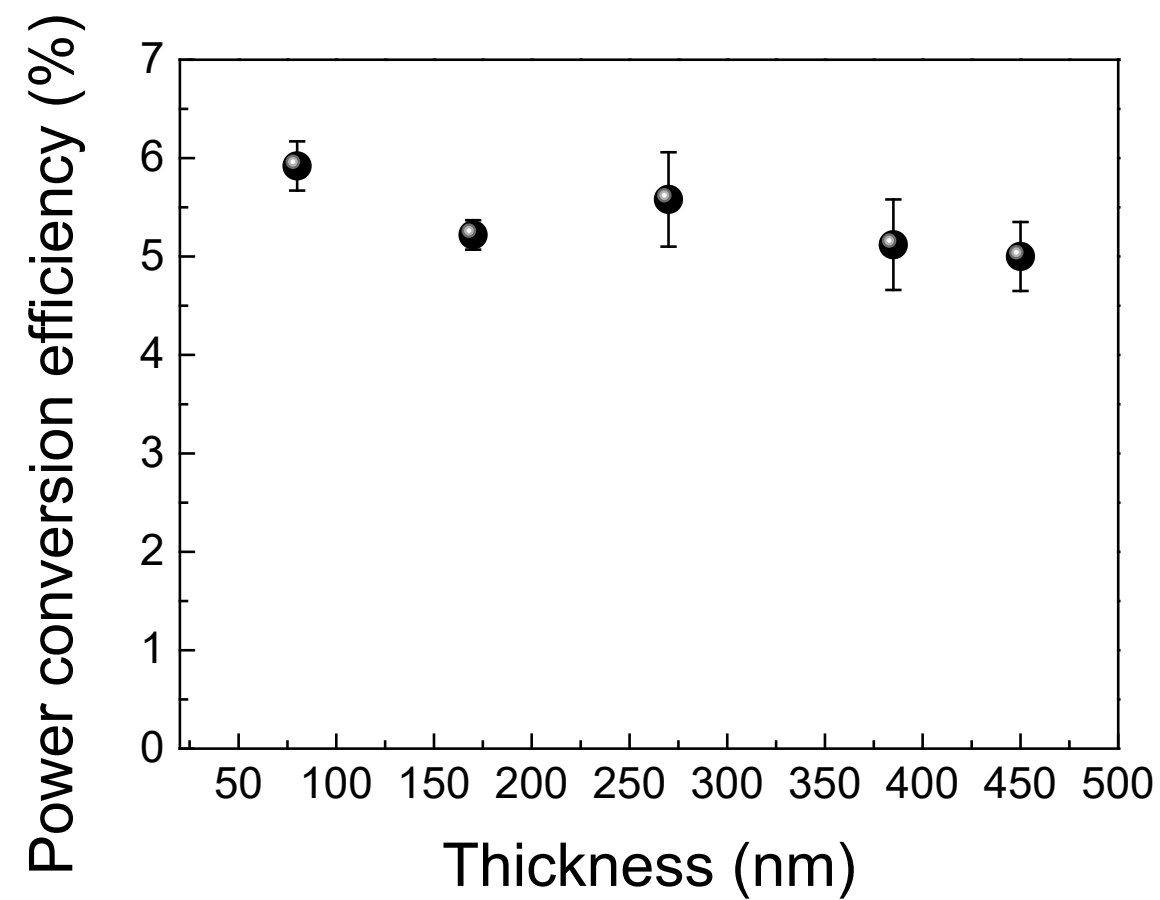
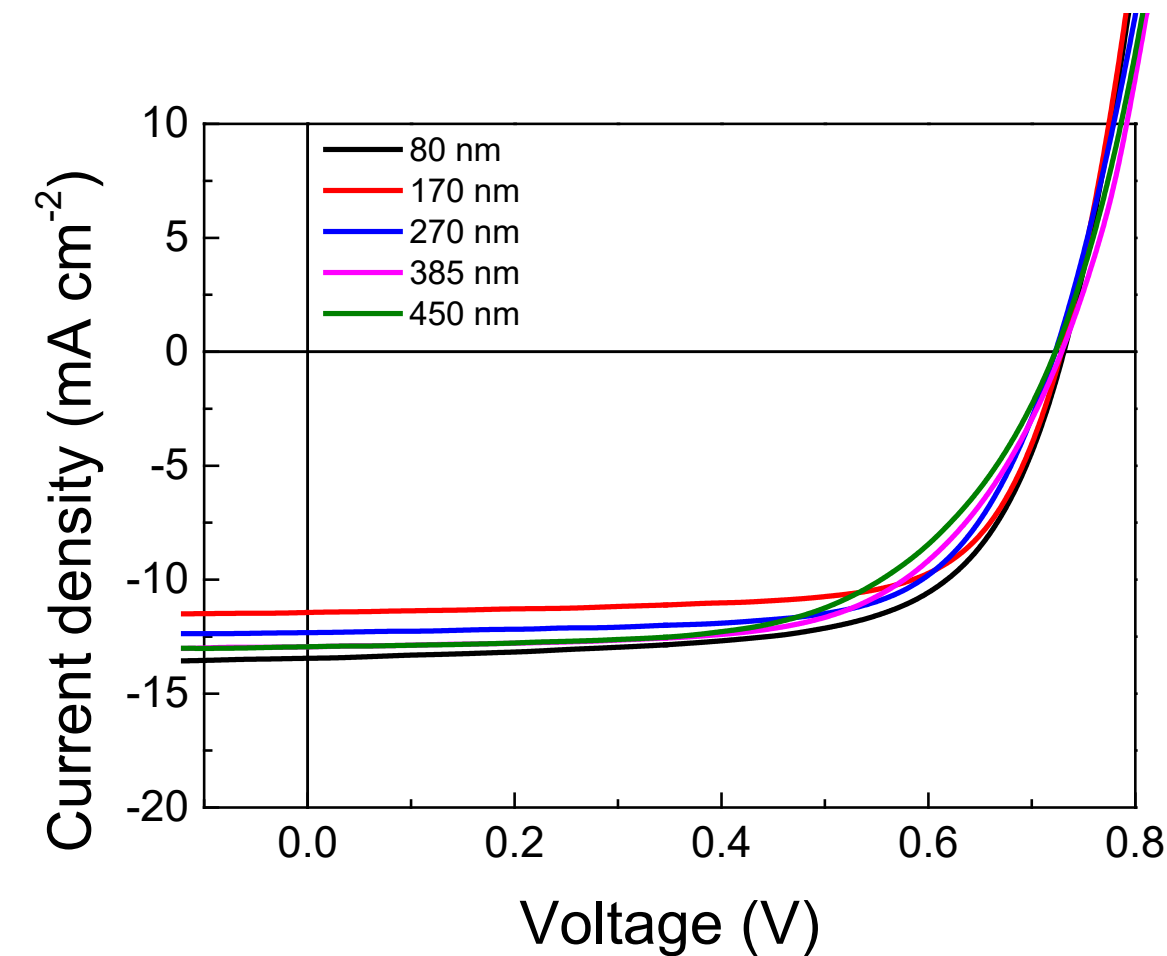


Transient Photovoltage

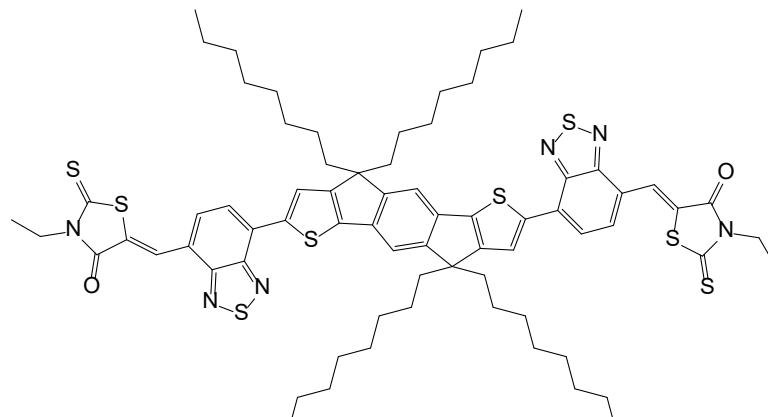


Longer charge carrier lifetime in P3HT:IDTBR

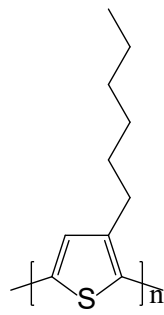
Thickness dependent JVs



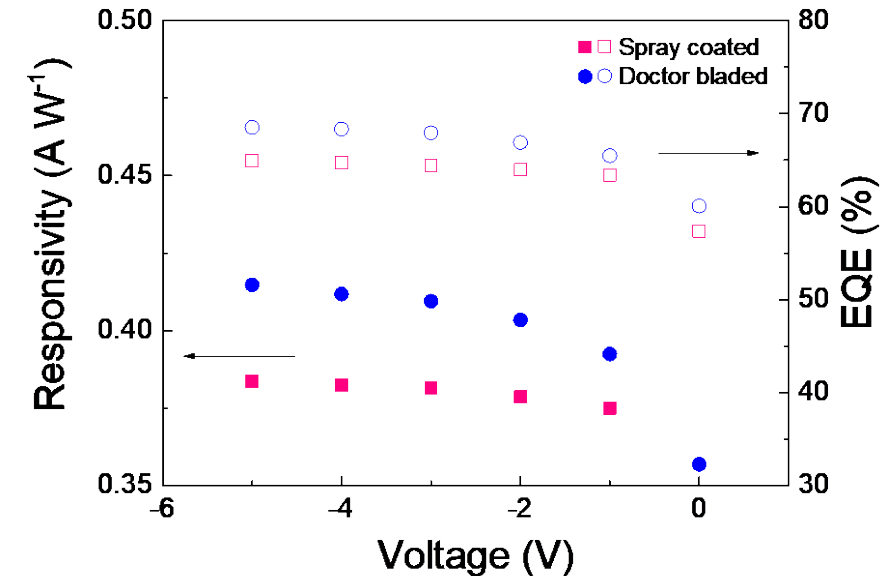
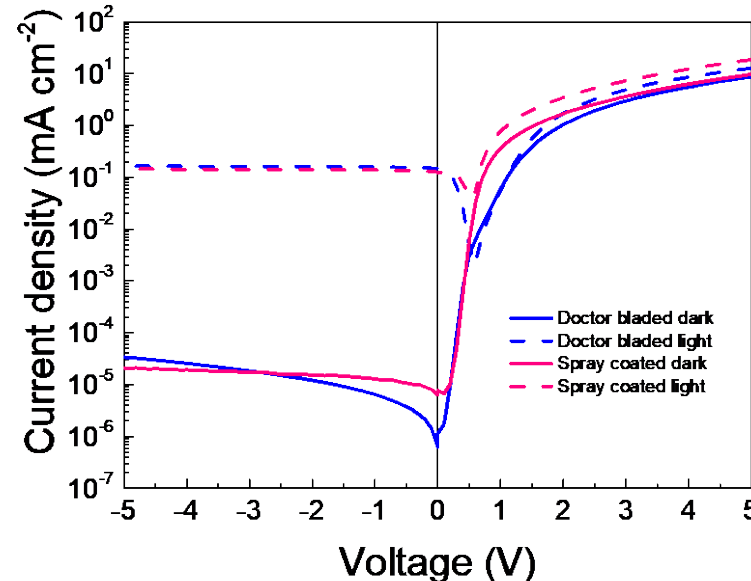
JVs and PD parameters



IDTBR

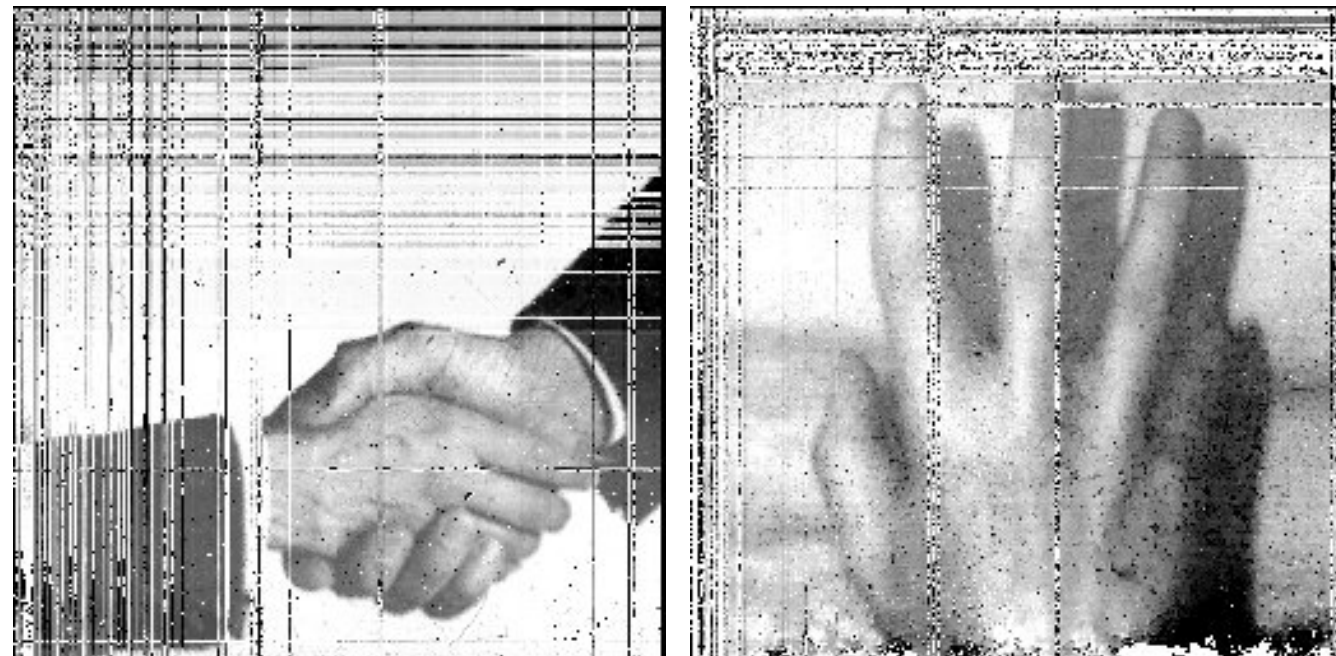
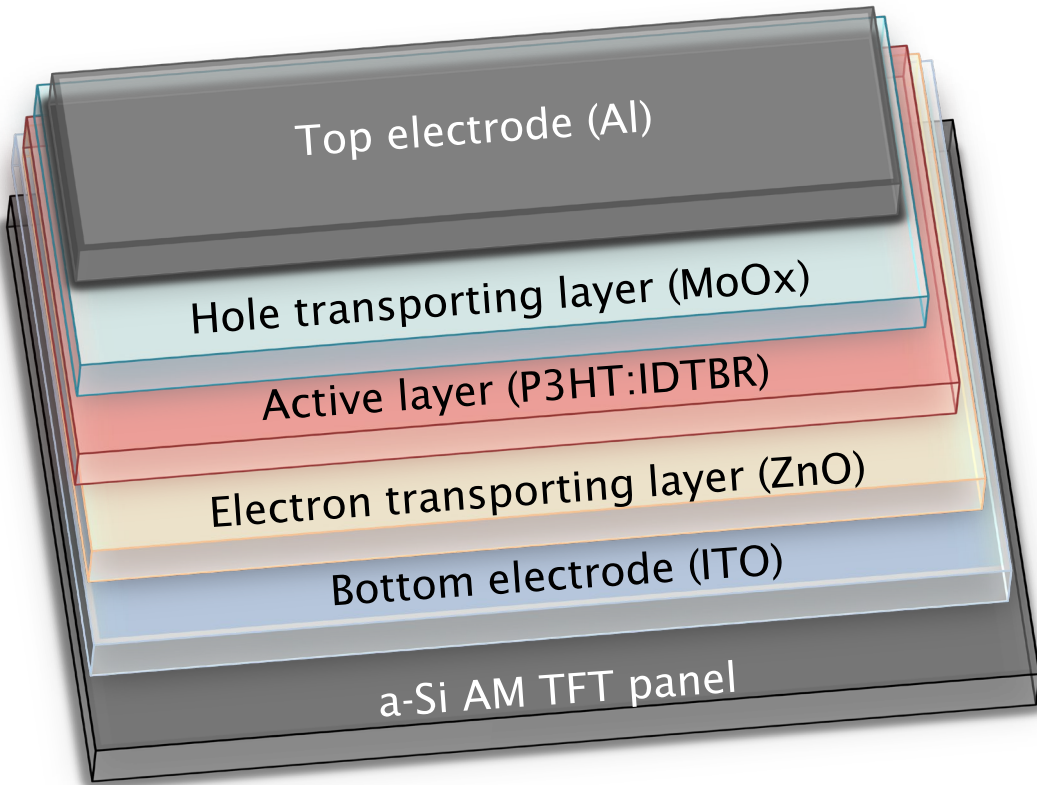


P3HT



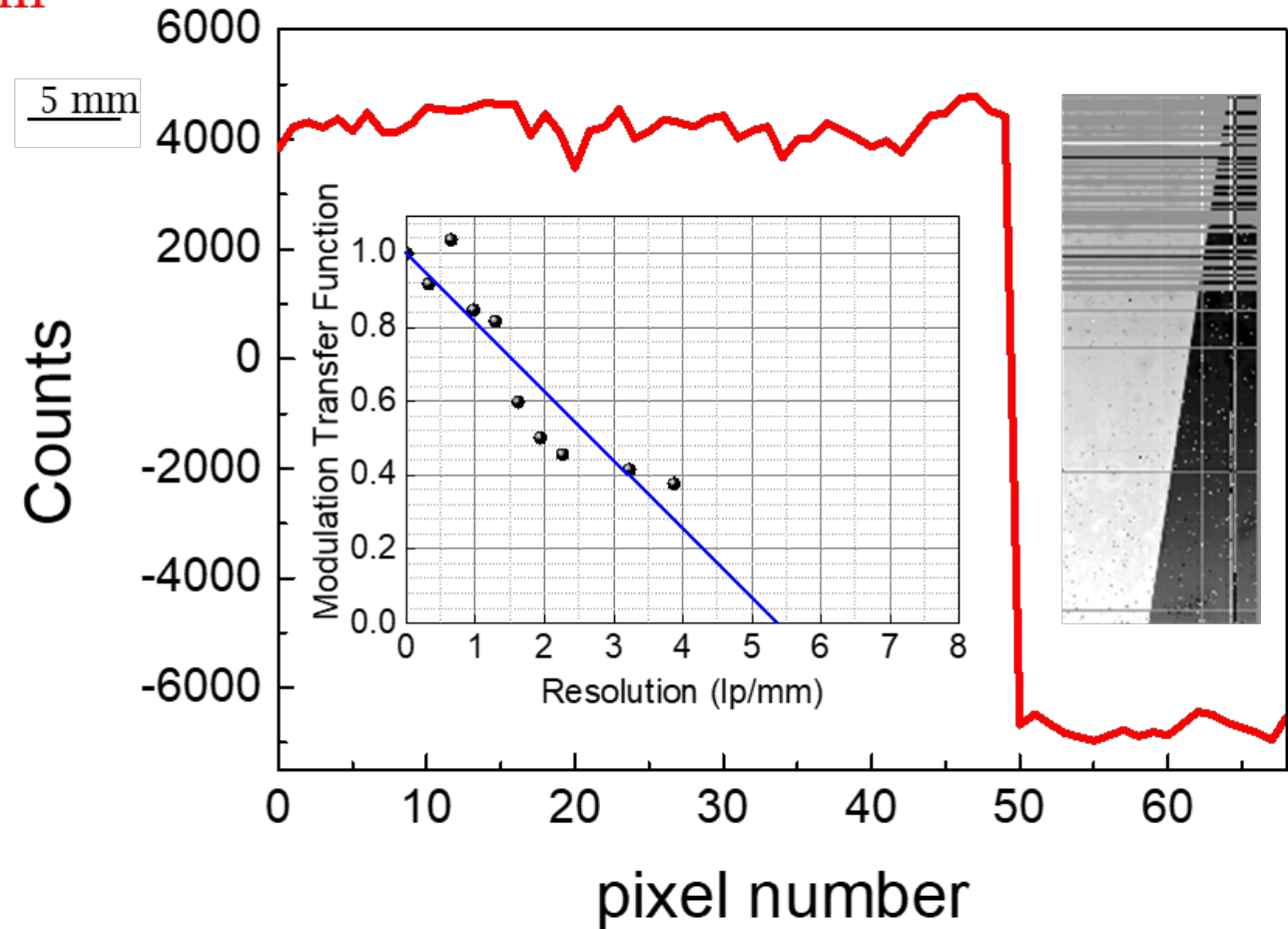
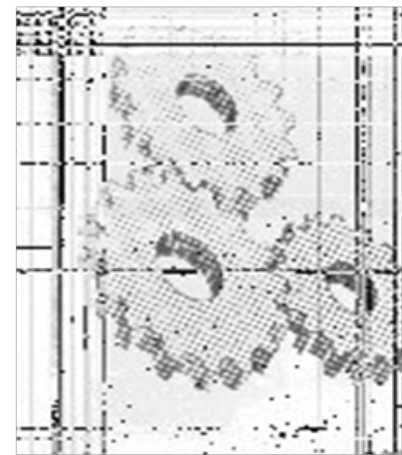
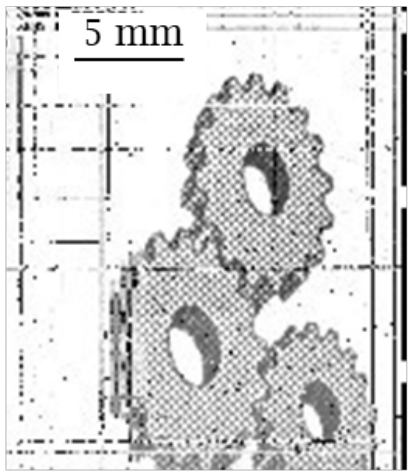
R [A W⁻¹]	f _{-3dB} [Hz]	f _{-6dB} [Hz]
0.42	52.6x10 ³	141.9x10 ³

Organic Photodetectors

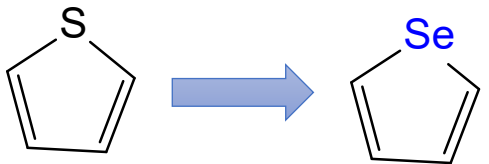


Imager characteristics

Green LED - 532 nm NIR LED - 850 nm

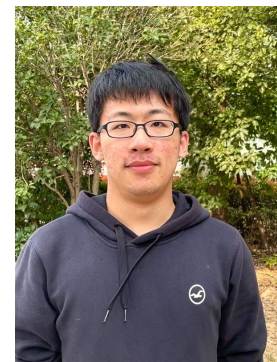
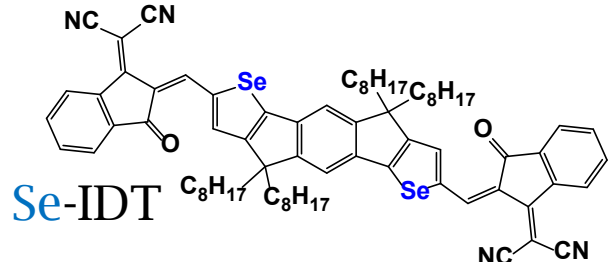
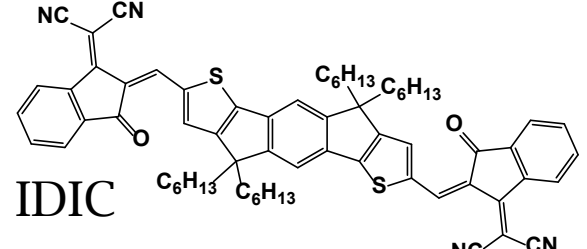


Selenium-Substituted NFA-IDSe

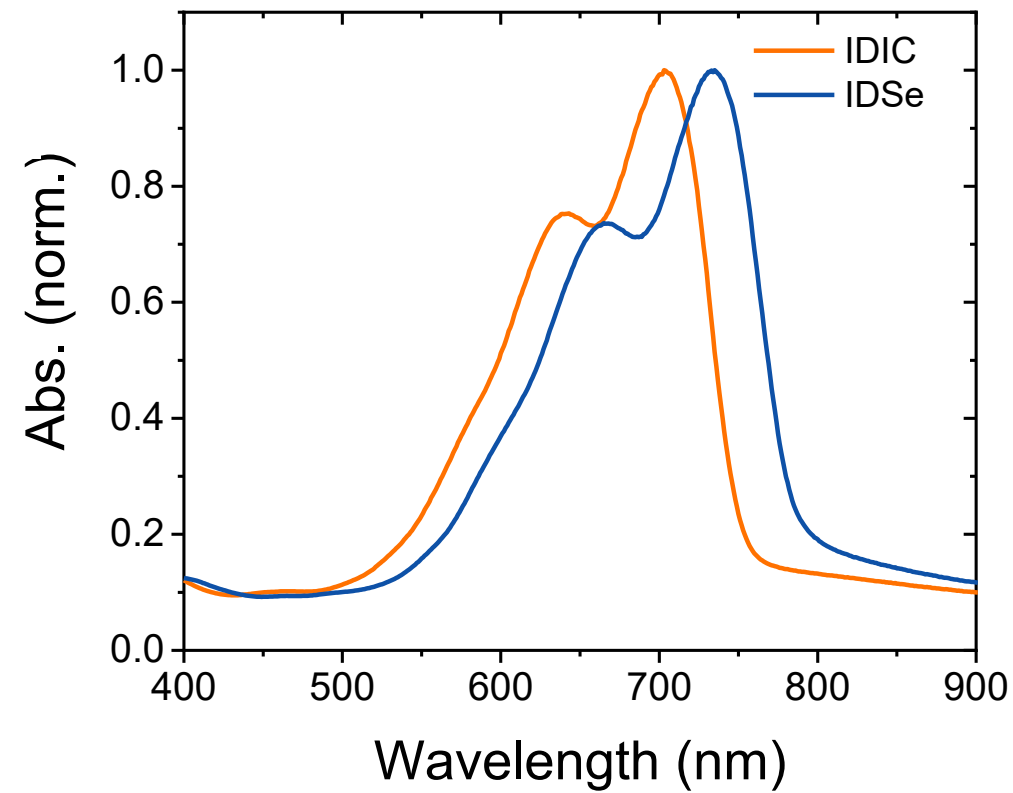


Lower aromatic stabilisation
Higher electron affinity
Increased polarisation

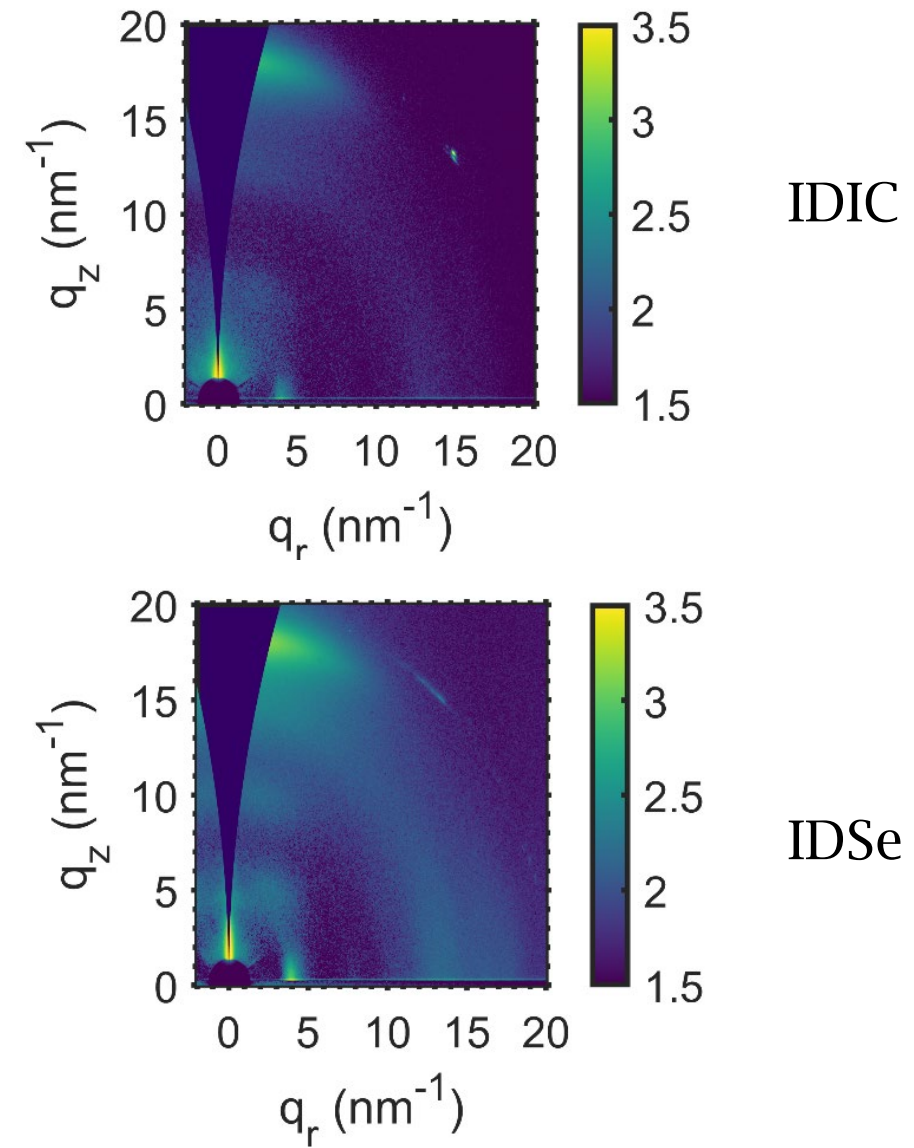
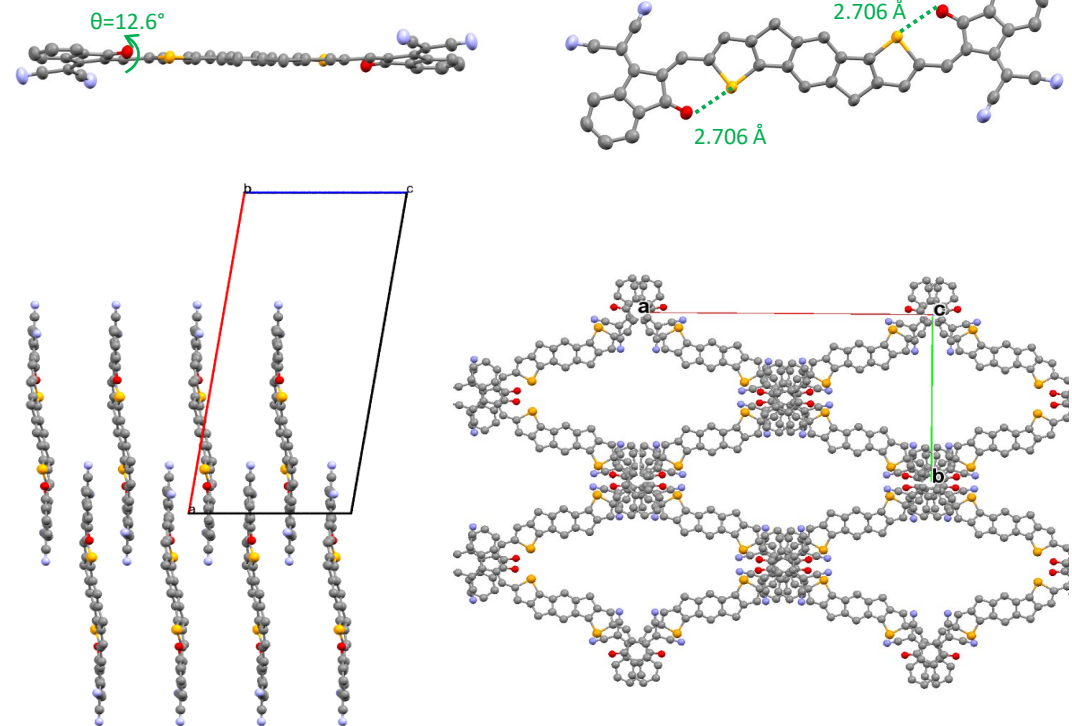
Reduced bandgap → red-shift absorption
Improved intermolecular interaction



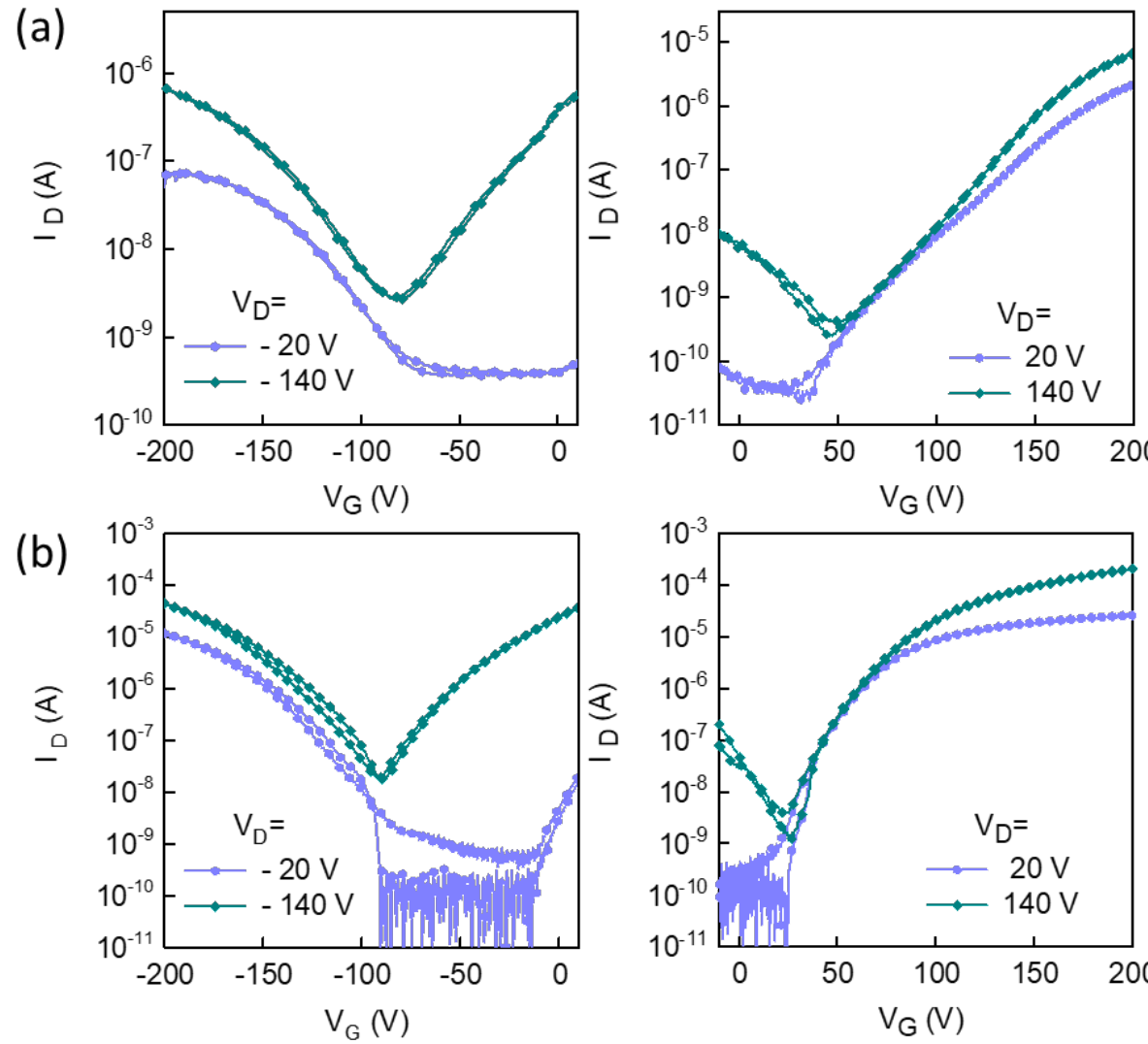
And the
Heeney group



Selenium-Substituted NFA-IDSe



Charge carrier mobility



IDIC

$$\mu_{\text{electrons}} = 0.002 \text{ cm}^2 \text{ V}^{-1} \text{ s}^{-1}$$

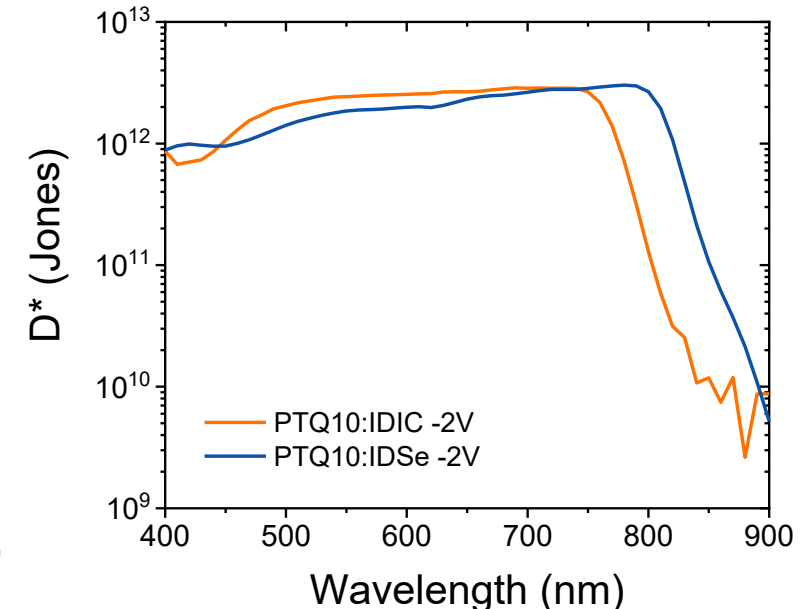
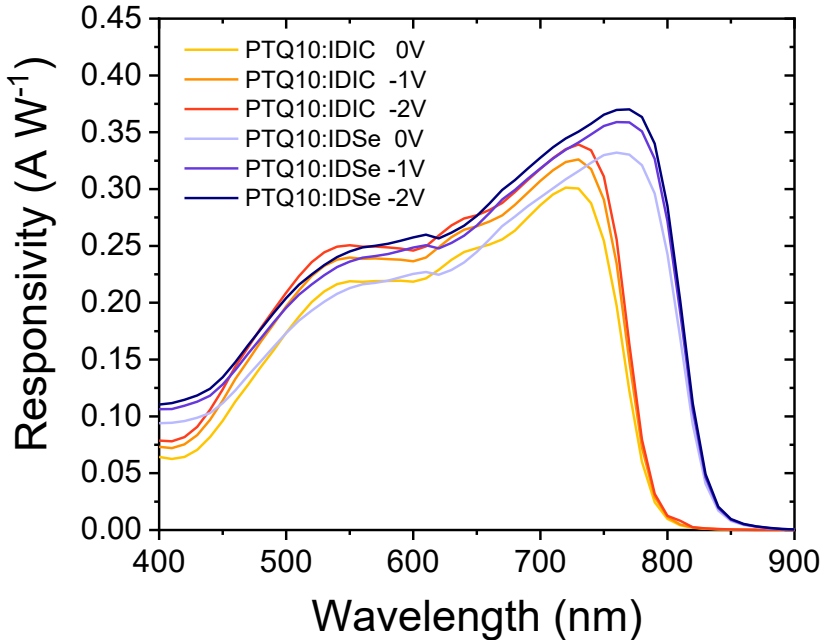
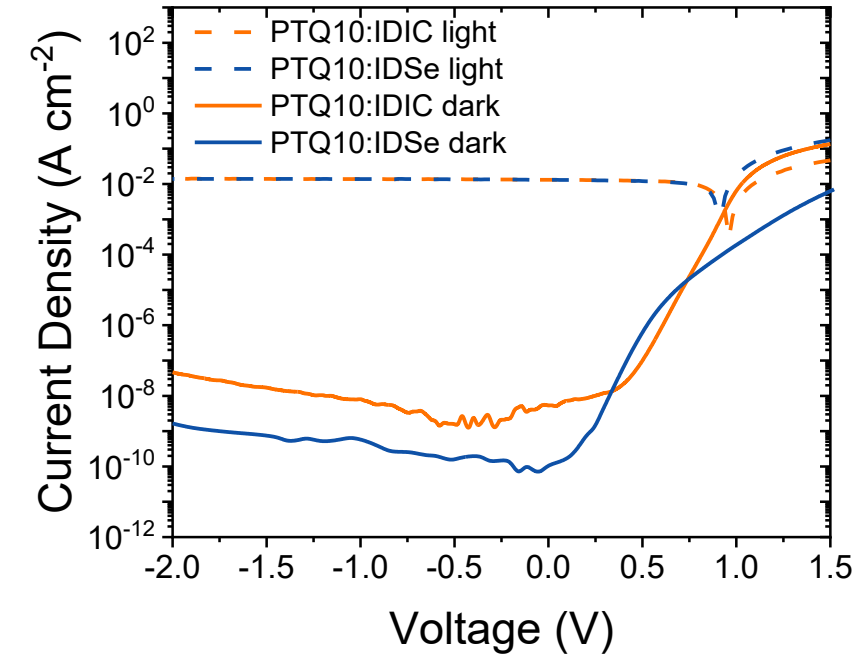
$$\mu_{\text{holes}} = 0.009 \text{ cm}^2 \text{ V}^{-1} \text{ s}^{-1}$$

IDSe

$$\mu_{\text{electrons}} = 0.16 \text{ cm}^2 \text{ V}^{-1} \text{ s}^{-1}$$

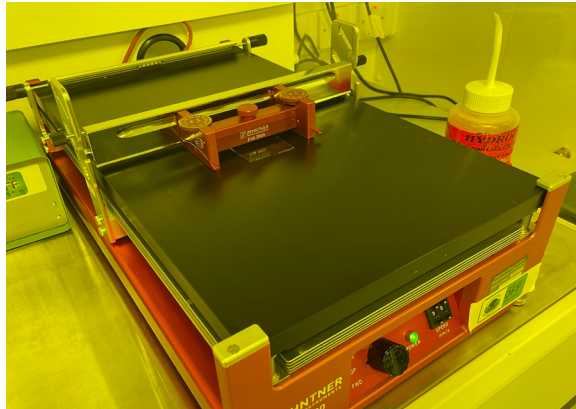
$$\mu_{\text{holes}} = 0.22 \text{ cm}^2 \text{ V}^{-1} \text{ s}^{-1}$$

Selenium-Substituted NFA-IDSe

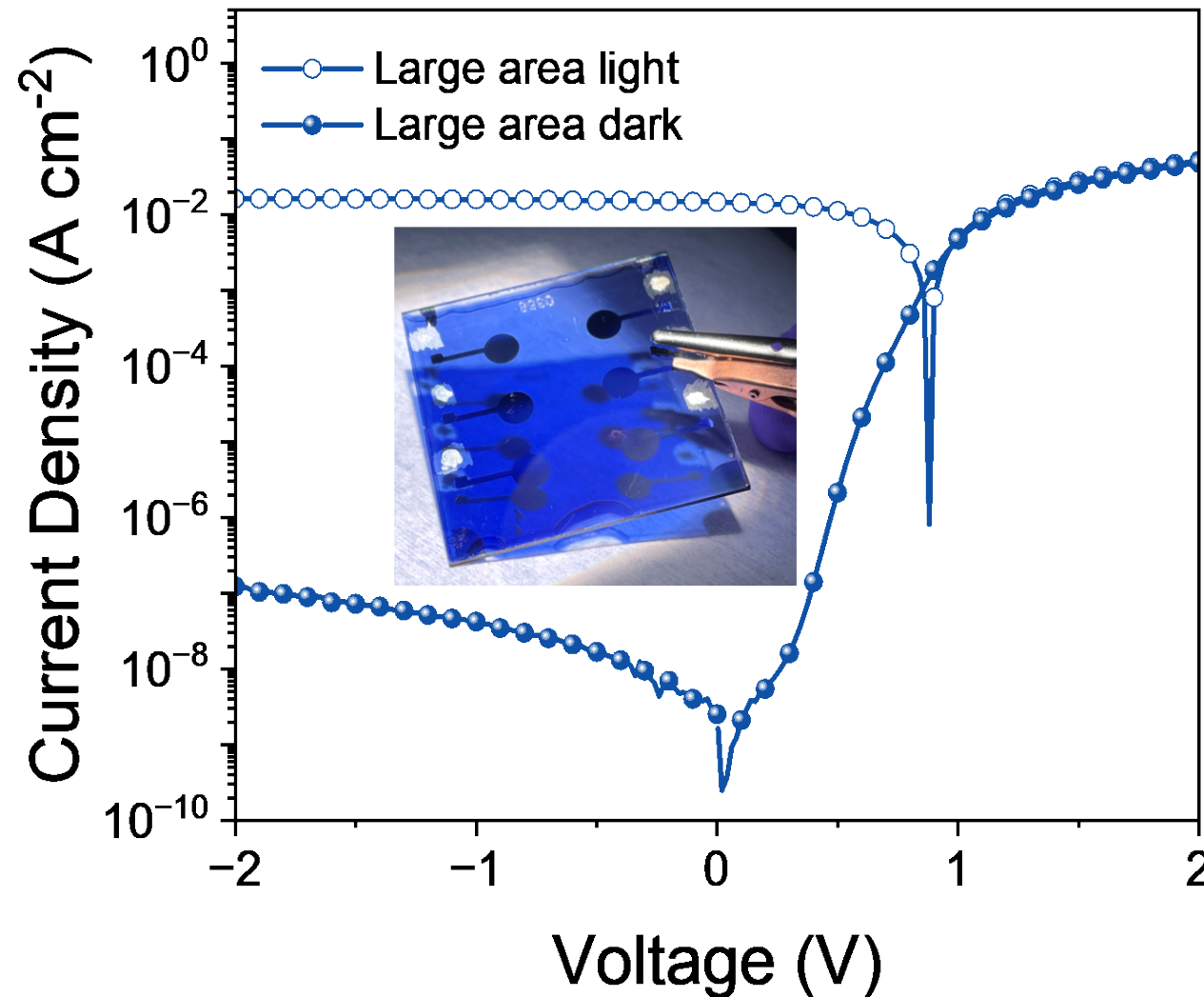


All figures of merit are higher in IDSe OPD

Blade coating- large-area device



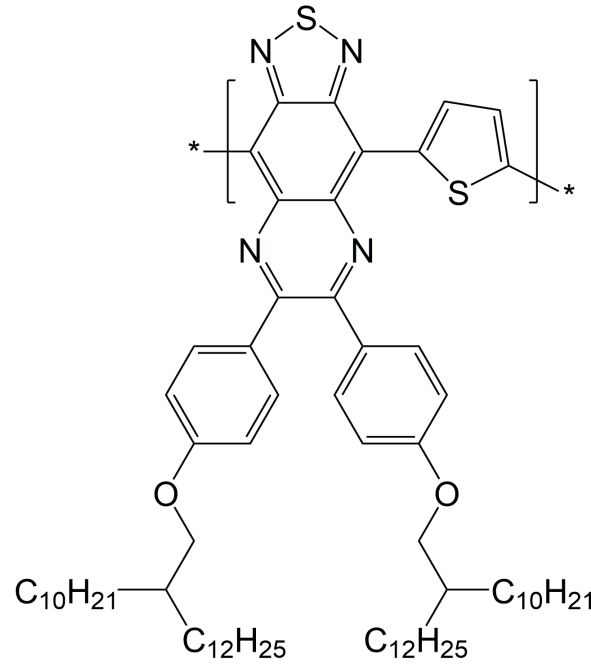
Dark current at -2V bias (A cm ⁻²)	
Large-area device	1.2×10^{-7}
Spin-coated device	1.7×10^{-9}



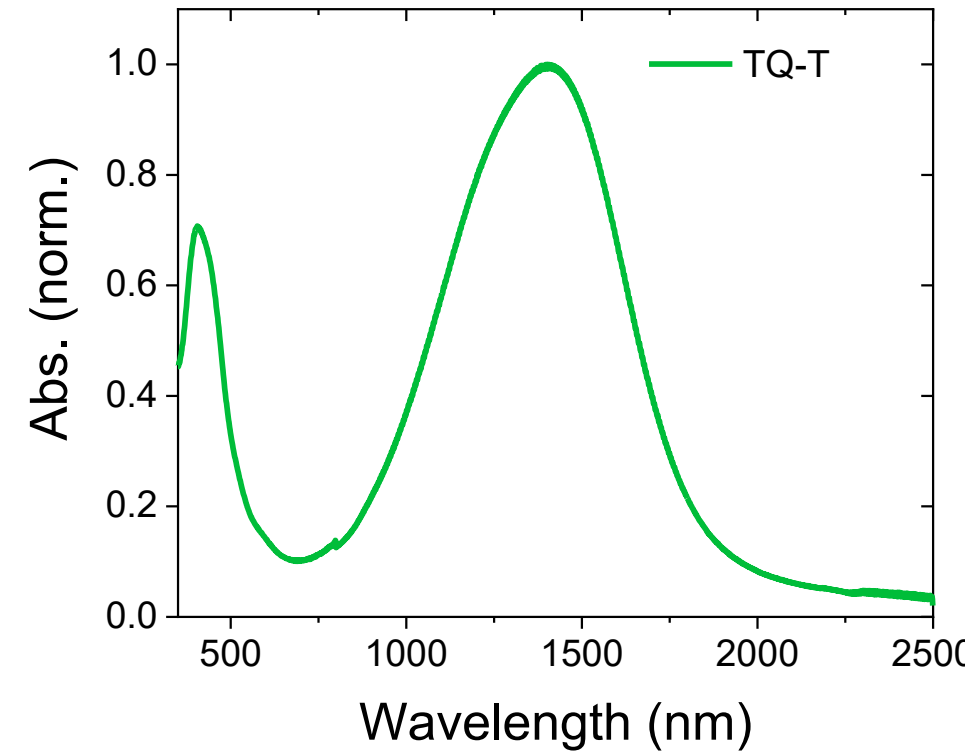
Ultra-low bandgap polymer for organic photodetector with high infrared detectivity

25

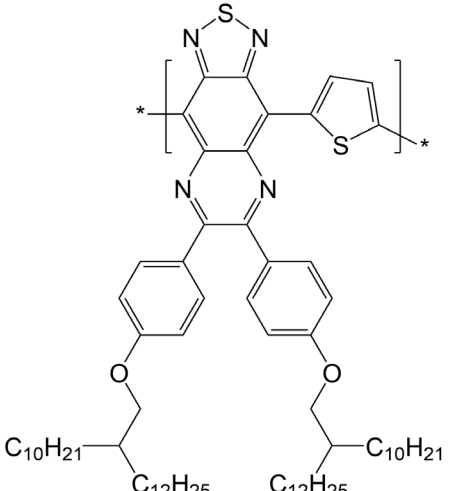
Imperial College
London



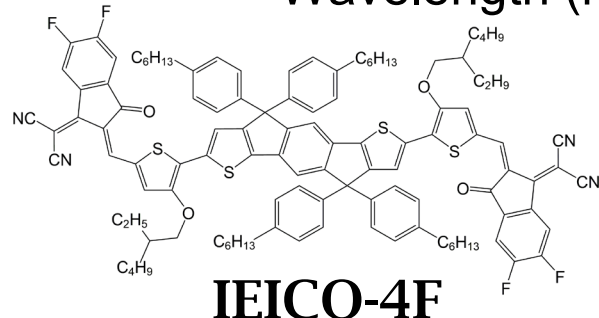
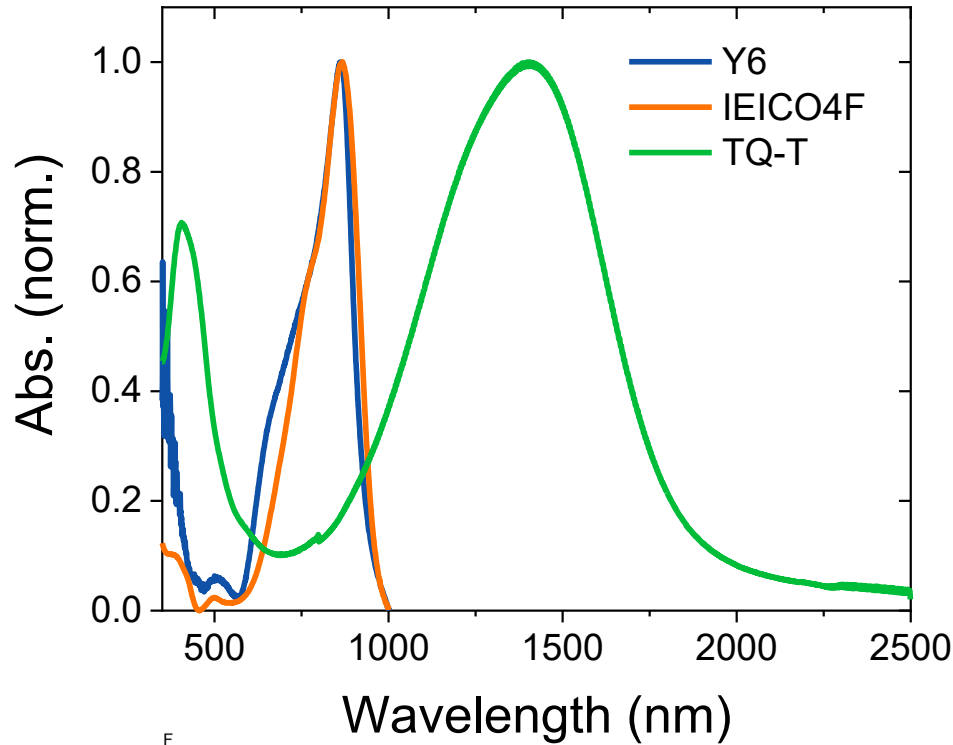
TQ-T



Ultra-low bandgap polymer for organic photodetector with high infrared detectivity



TQ-T



IEICO-4F

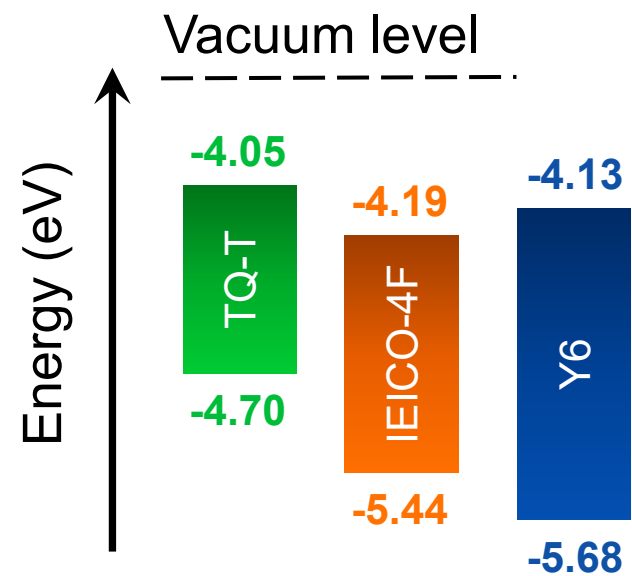
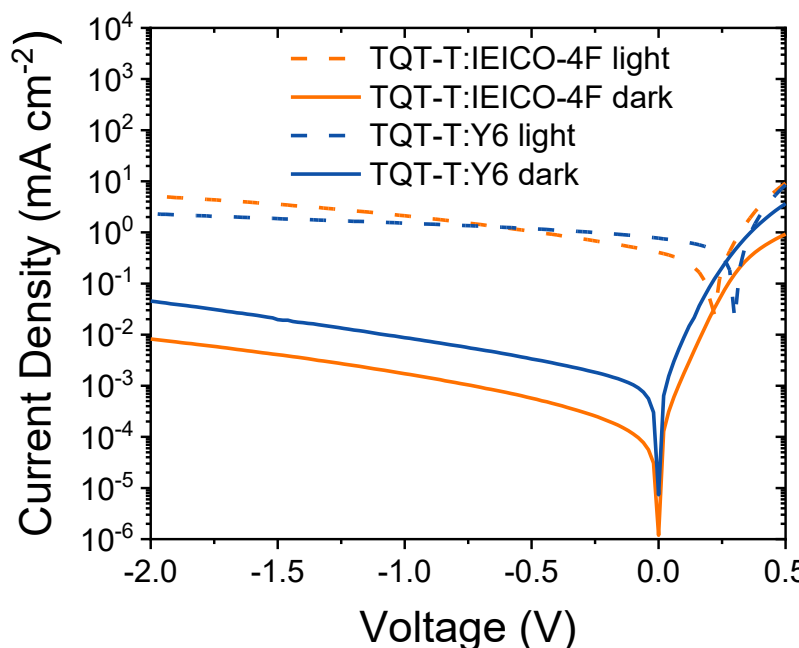
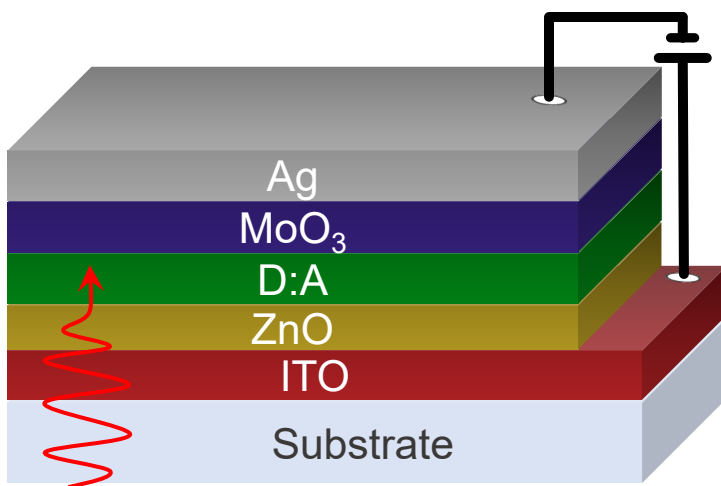
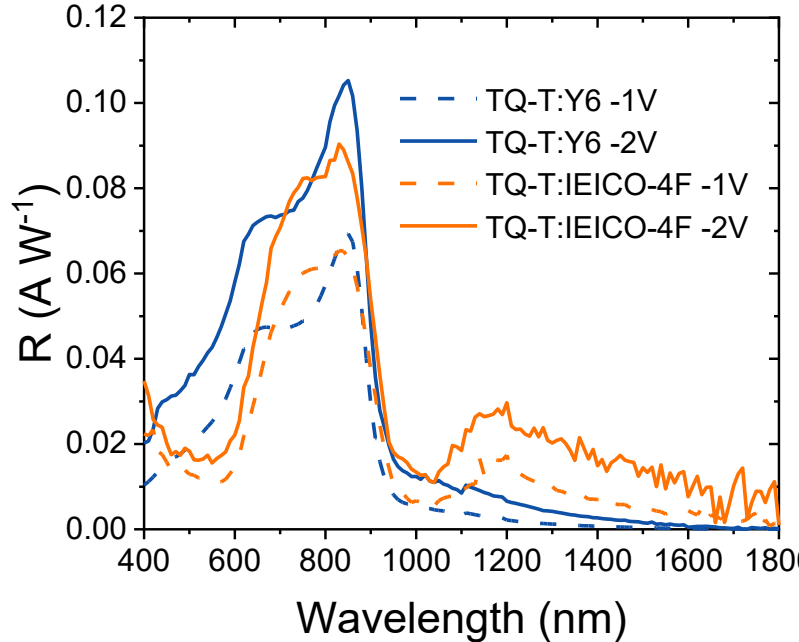


Figure of Merits

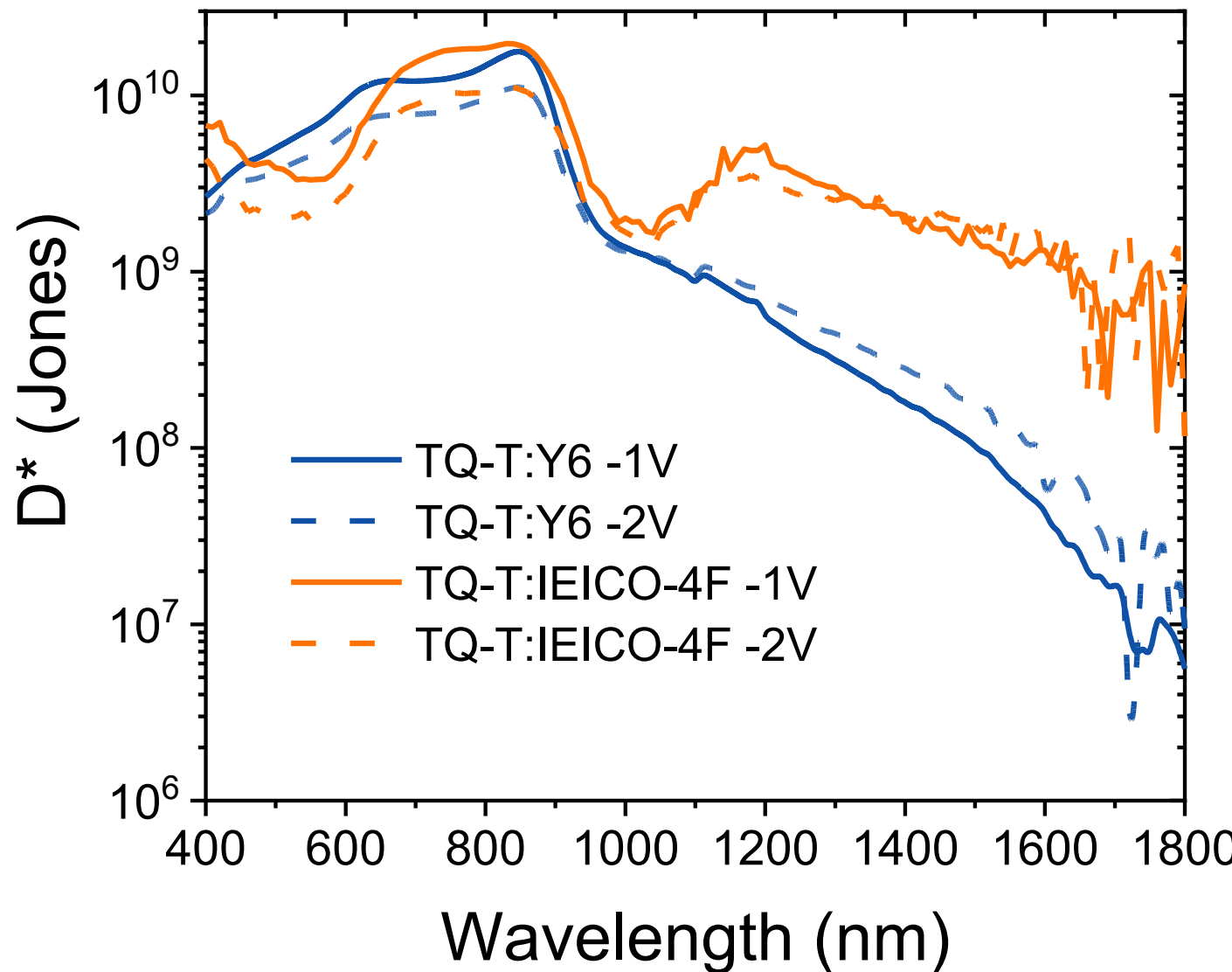


J_d at -2 V of $8.4 \times 10^{-3} \text{ mA cm}^{-2}$



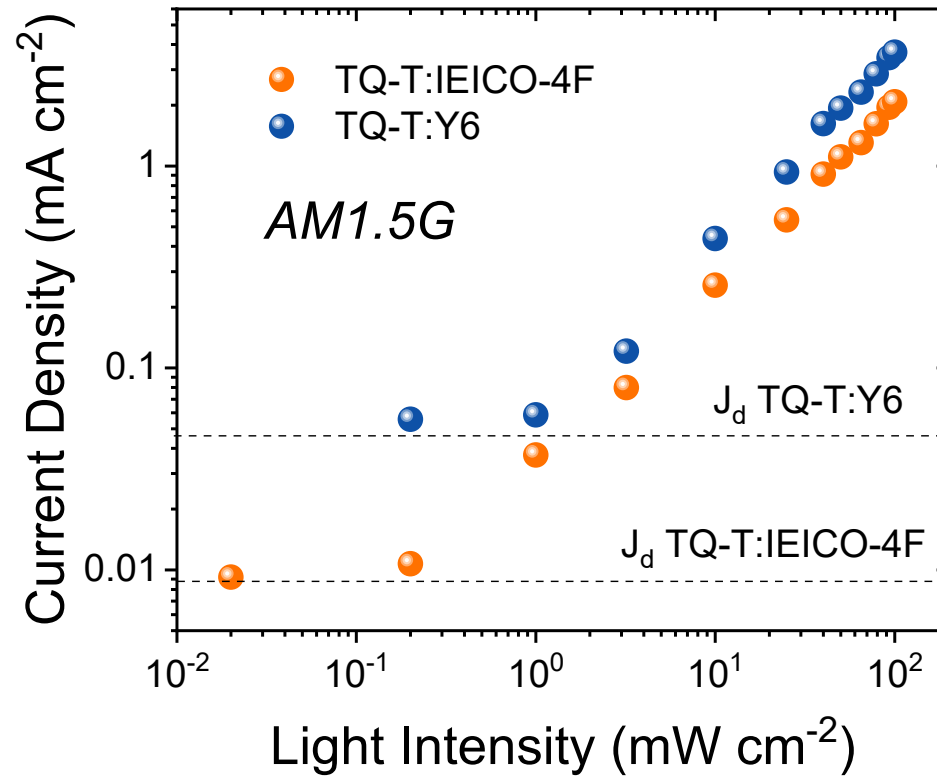
R at -2 V of 0.03 A W^{-1}
(EQE 2%)

Specific Detectivity



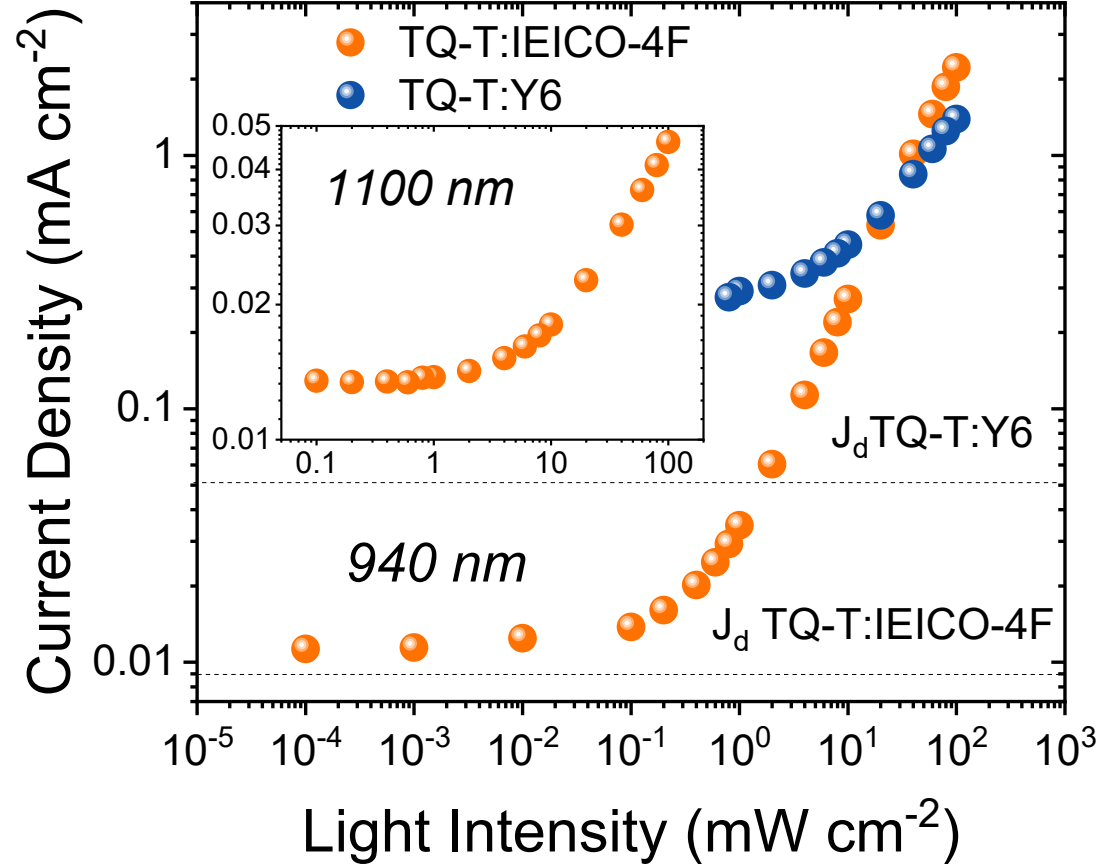
TQ-T:IEICO-4F OPD D* of 10^9 - 10^{10} Jones in the UV-Vis-NIR range

D* calculated from NEP and not Jd!

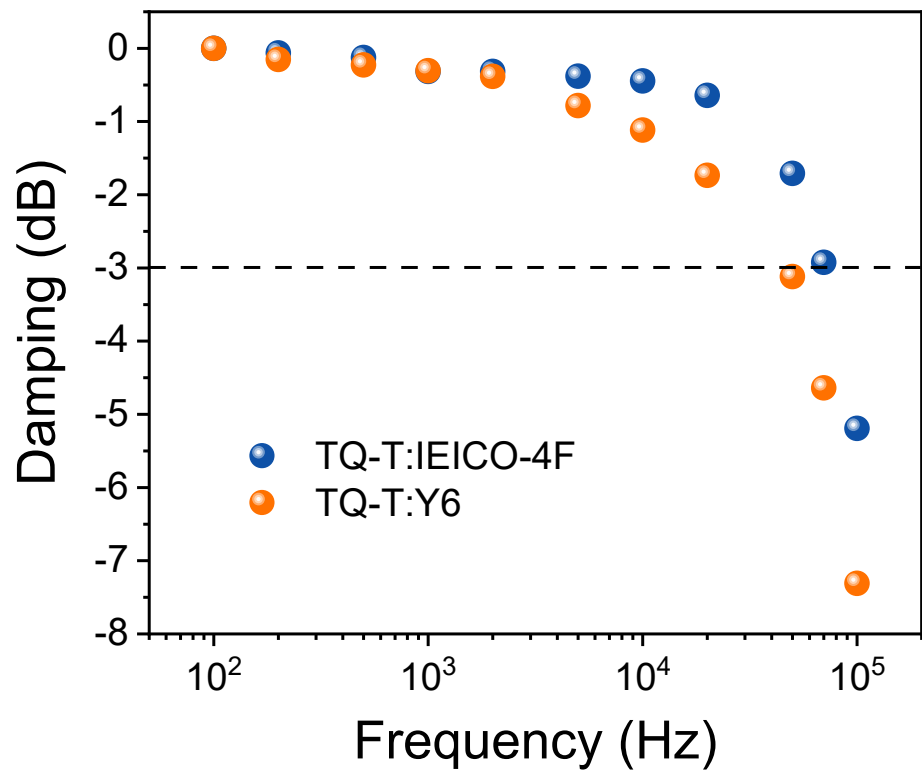


TQ-T:IEICO-4F 45.8 dB

TQ-T:Y6 35.7 dB

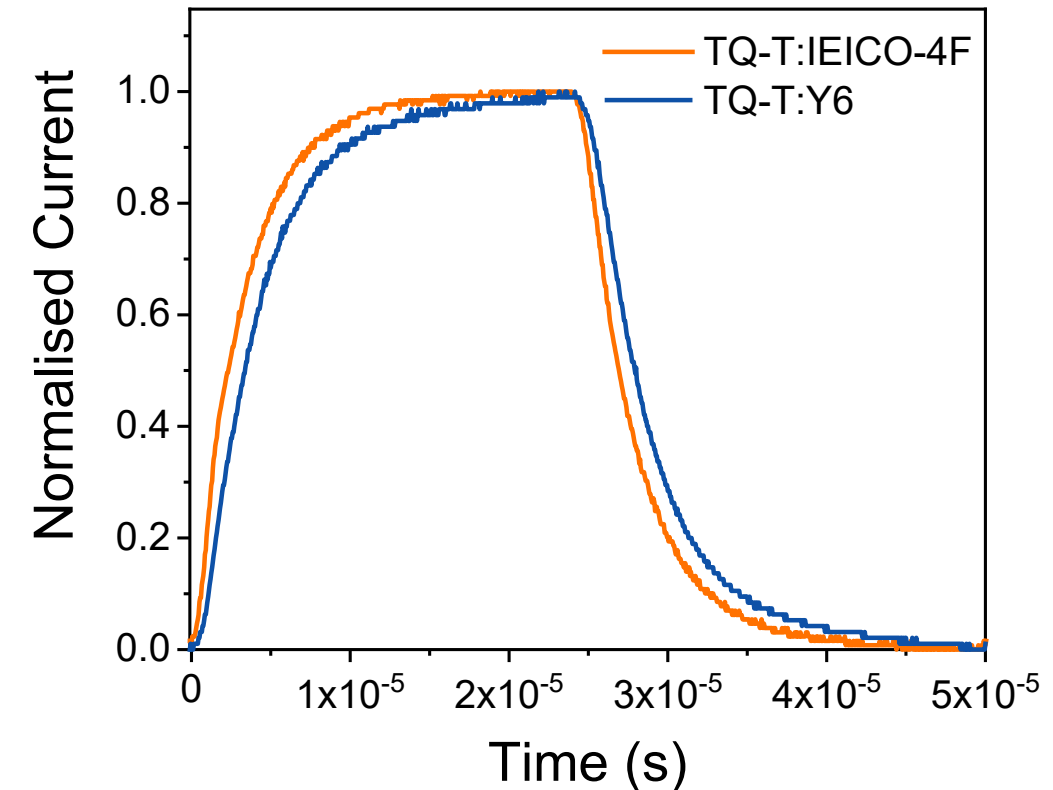


Charge dynamics



TQ-T:IEICO-4F 100 kHz

TQ-T:Y6 90 kHz

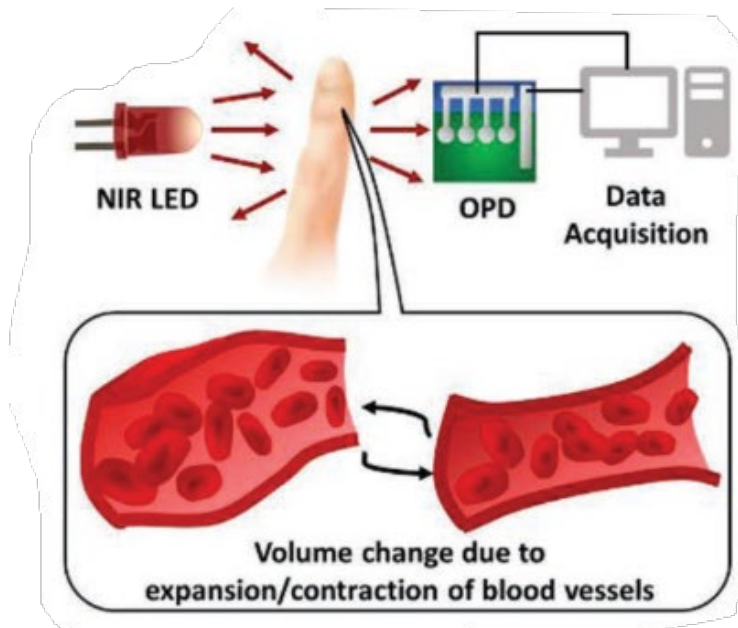


TQ-T:IEICO-4F rise/fall time 6.6/7.2 μ s

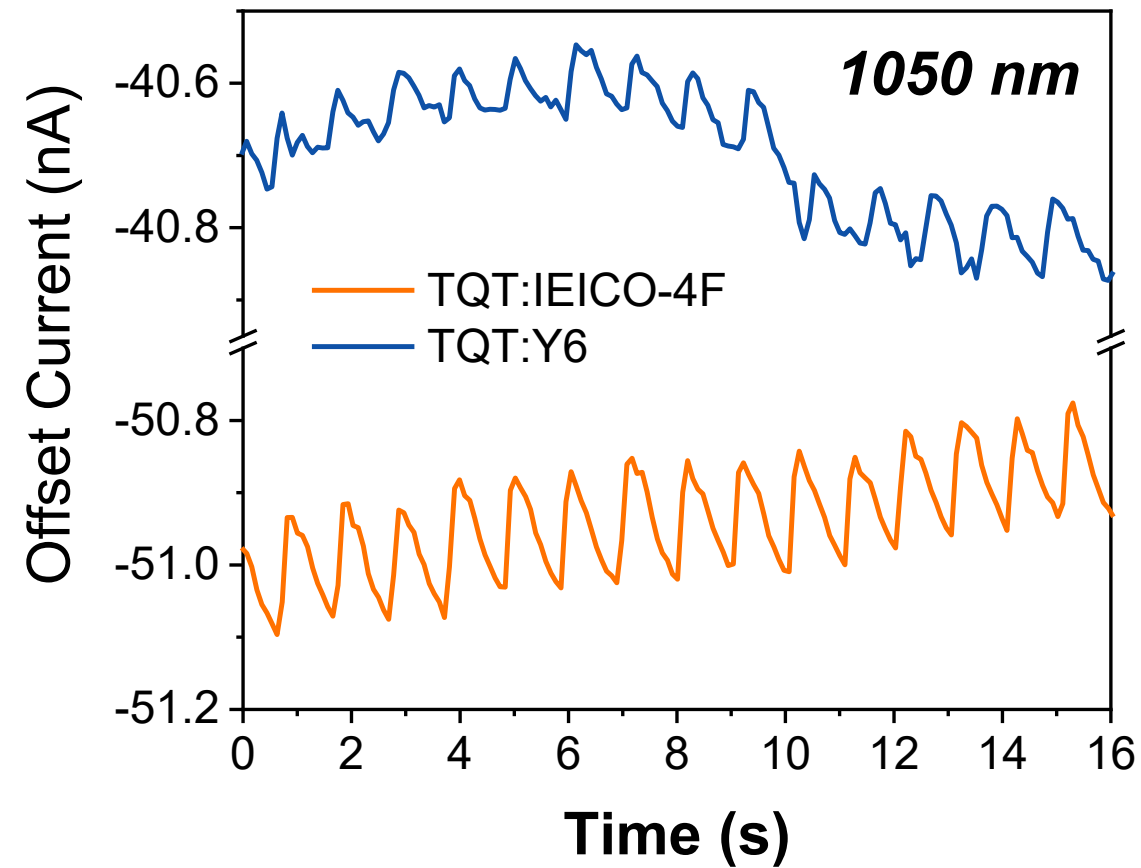
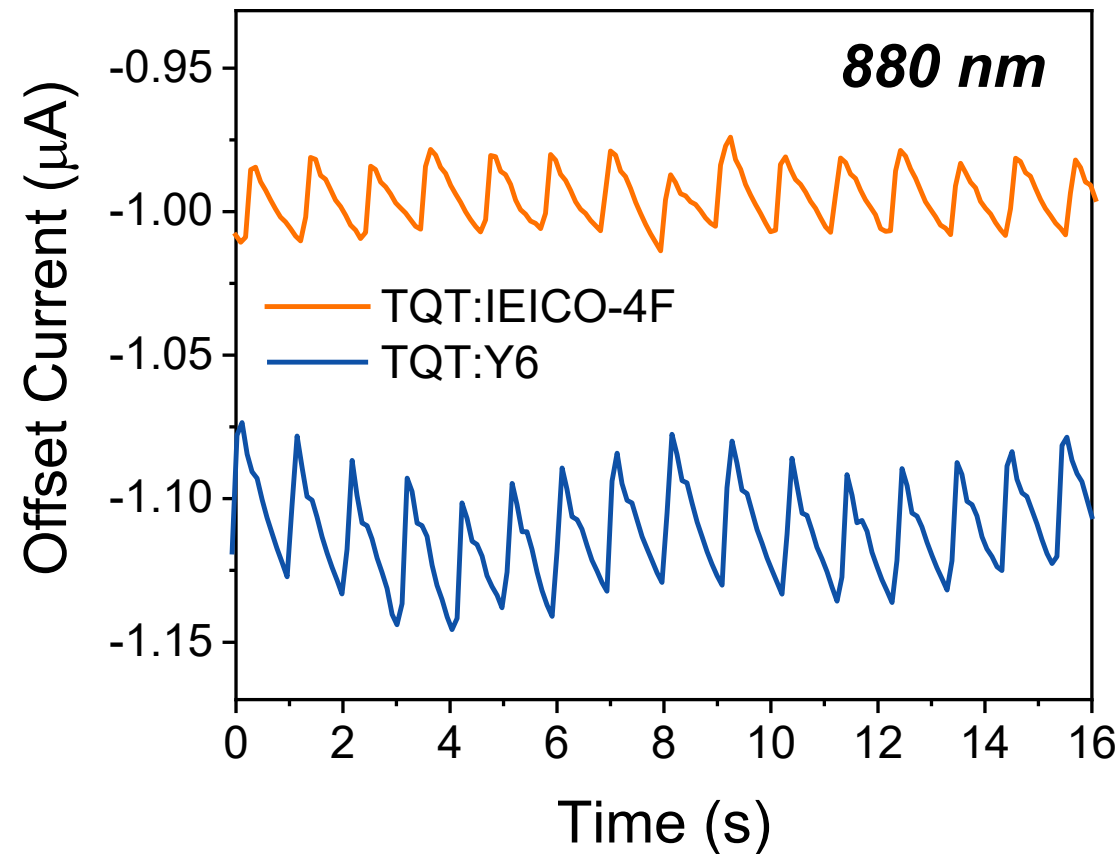
TQ-T:Y6 rise/fall time 7.3/8.3 μ s

Homemade Photoplethysmography setup

- **Photoplethysmography:** no-contact optical technique to detect volumetric changes in blood.
- Changes in absorbance → **direct current readout** from photodetector.

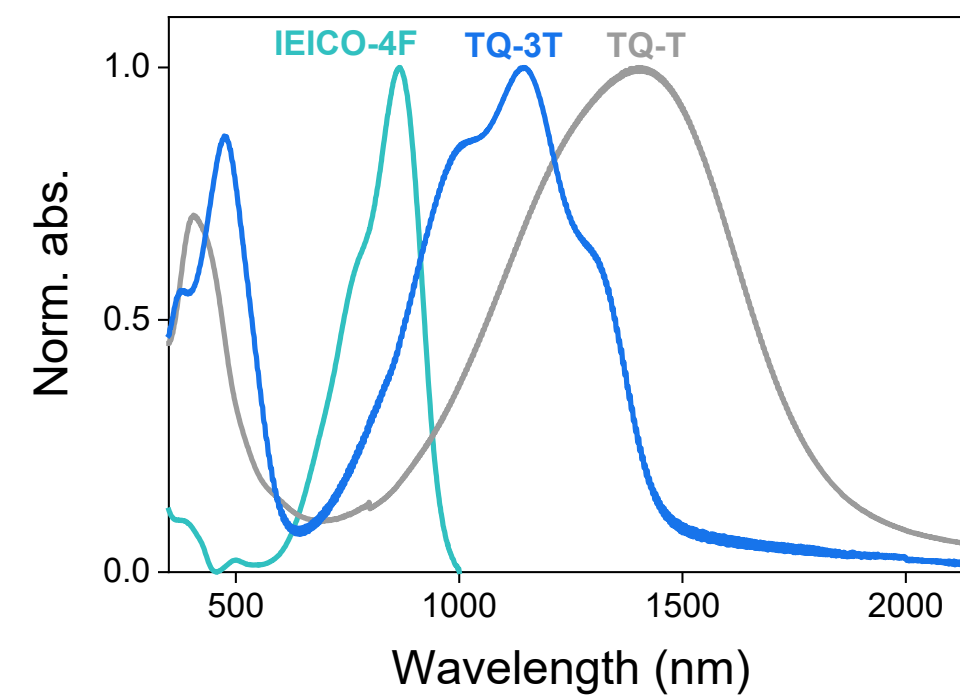
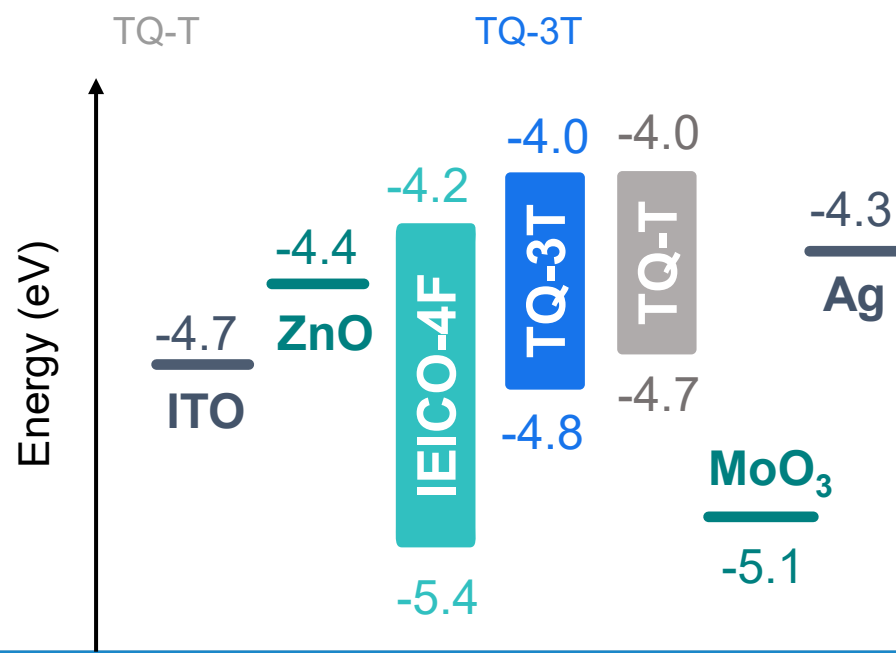
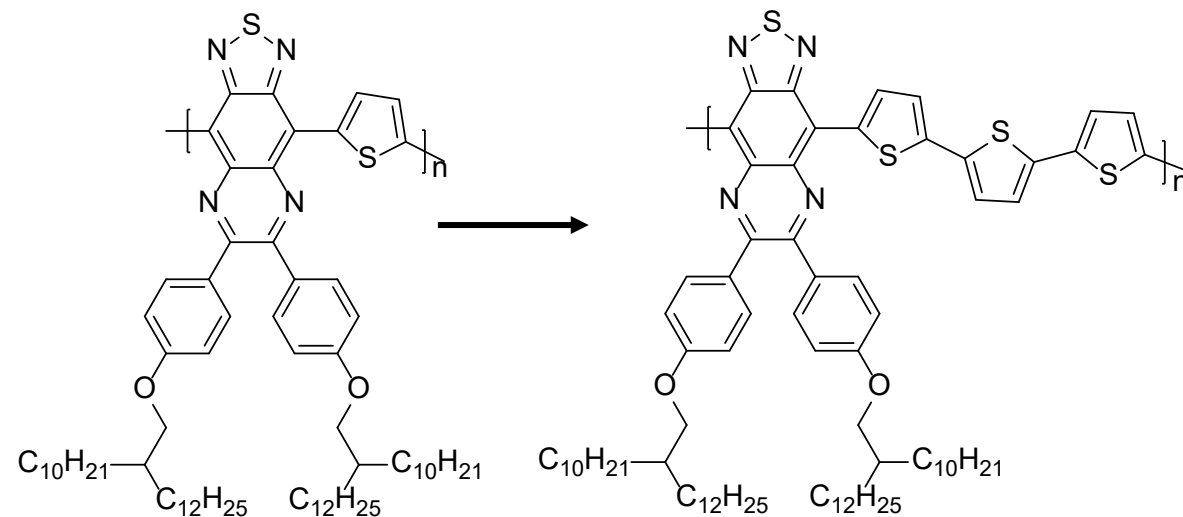


HB monitoring - comparison

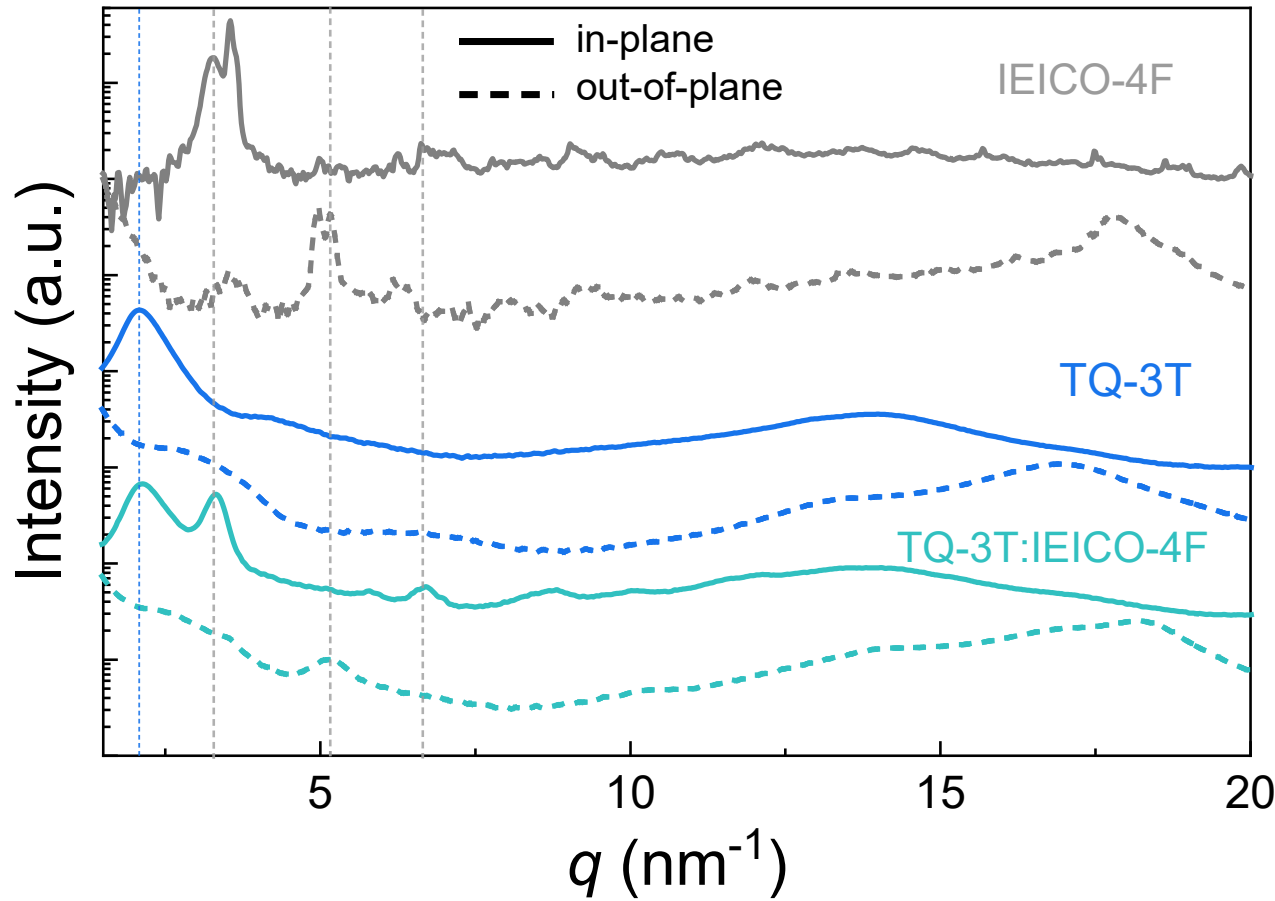
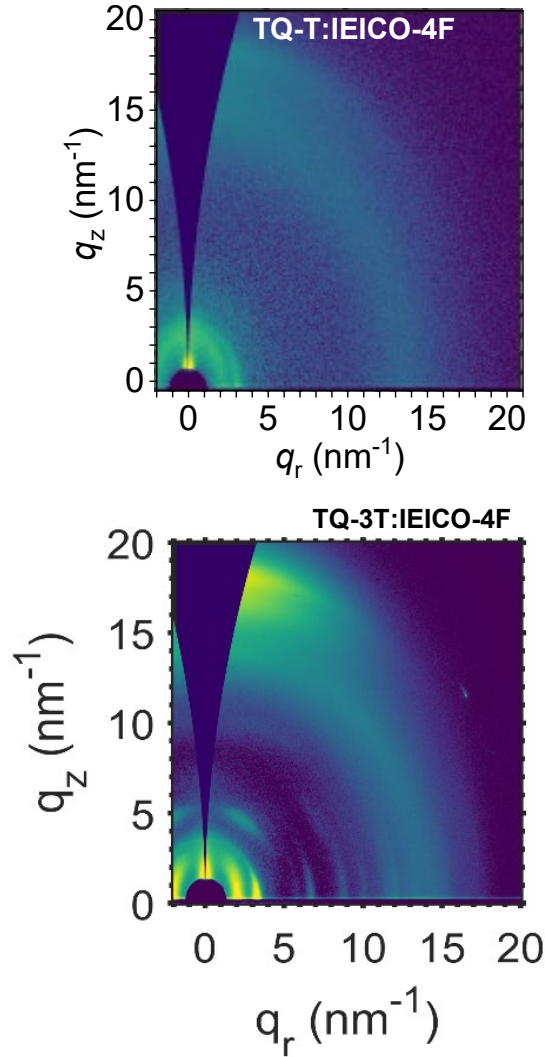


Tuning the polymer energetics

35

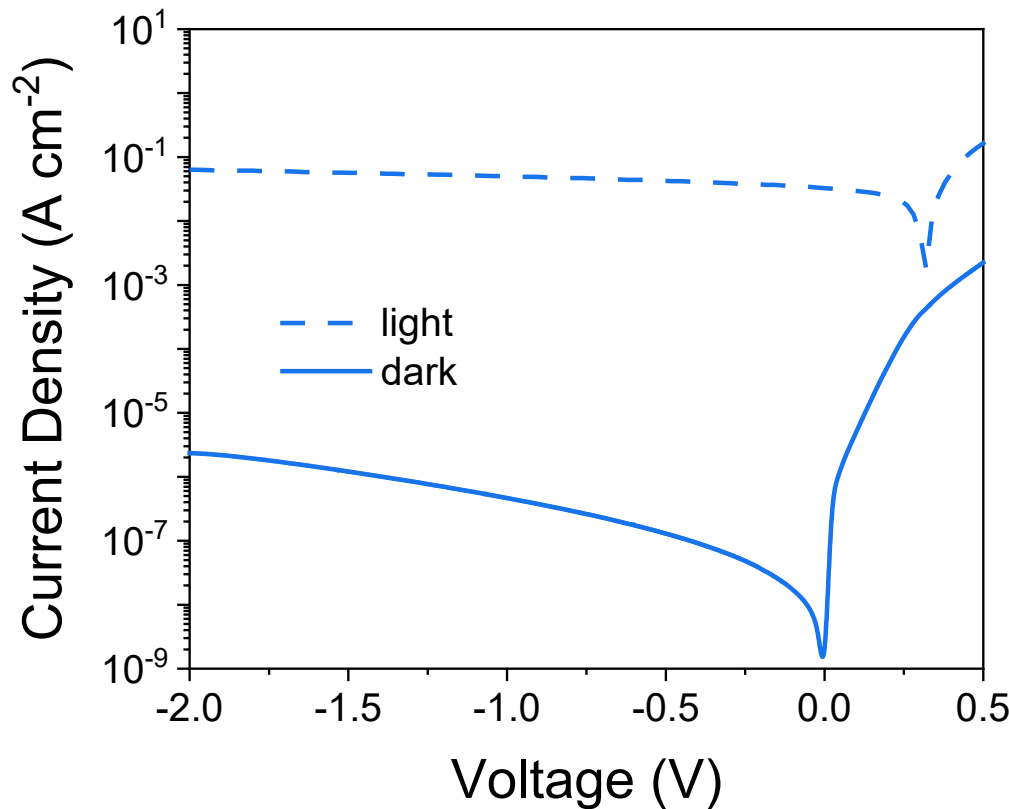
Imperial College
London

Tuning the polymer energetics and morphology

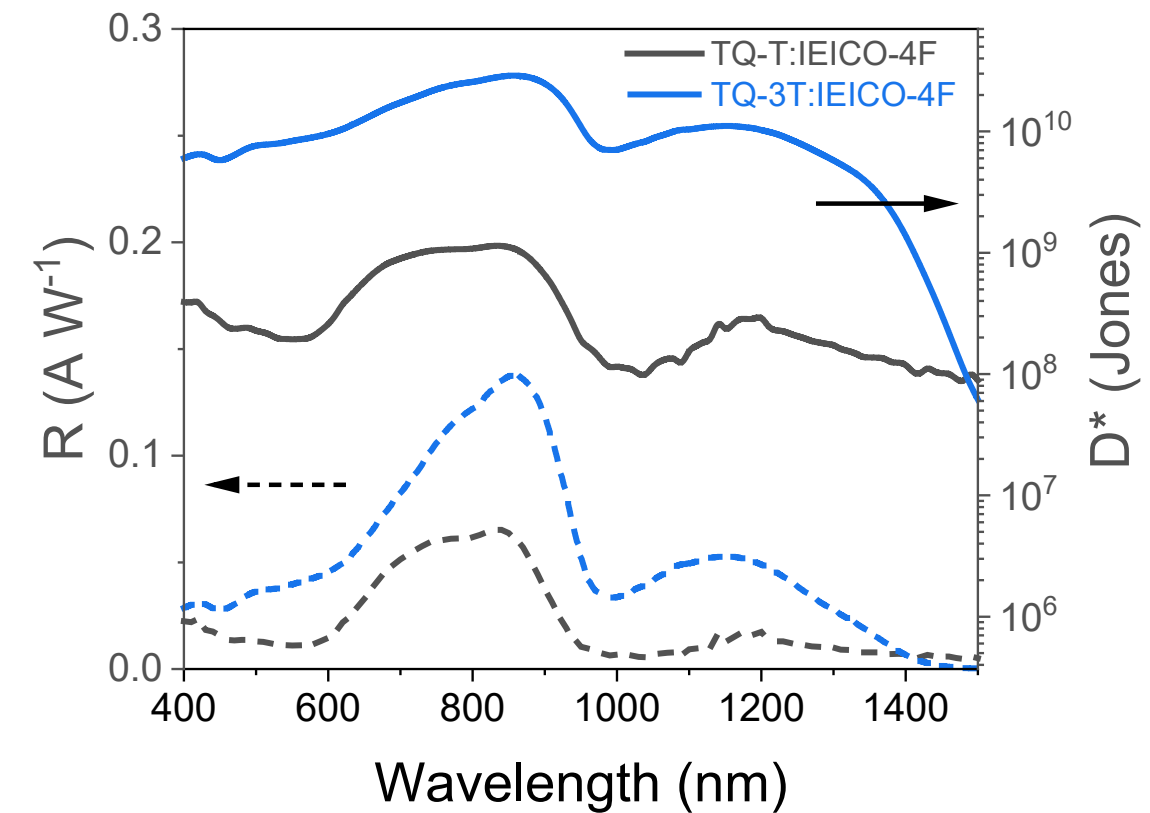


Improved microstructure in TQ-3T:IEICO-4F

Device performances

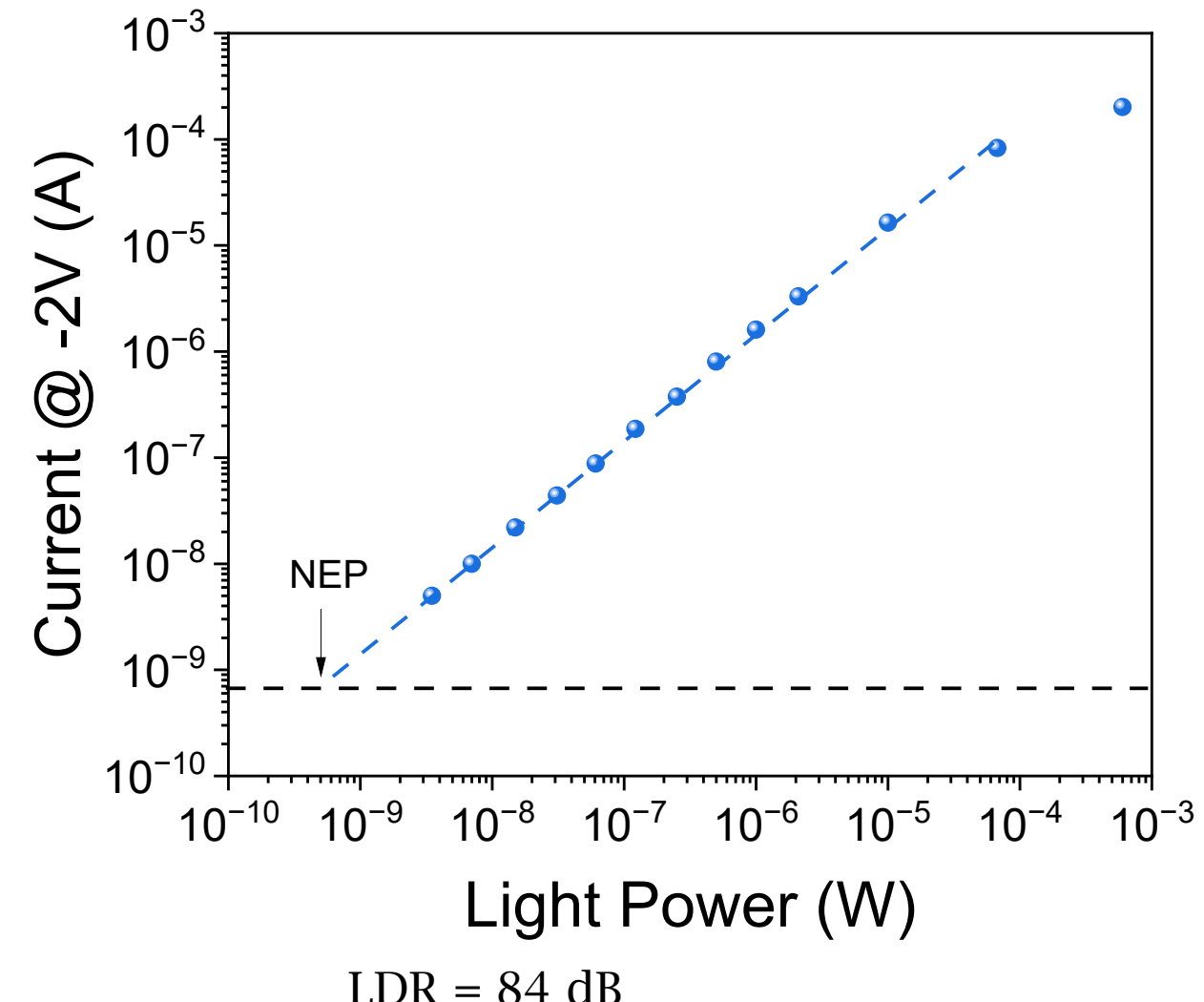
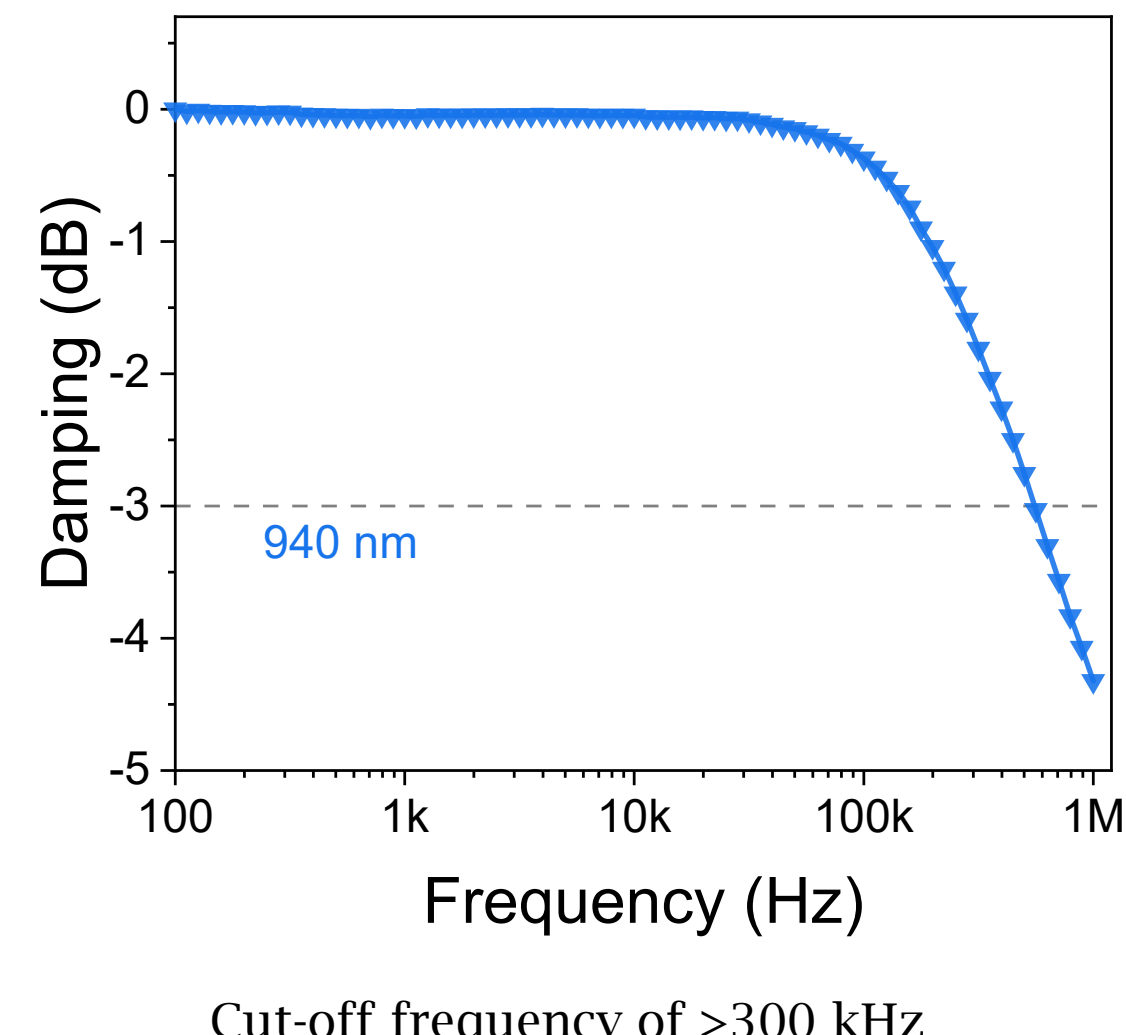


Jd reduced by 1 order of magnitude

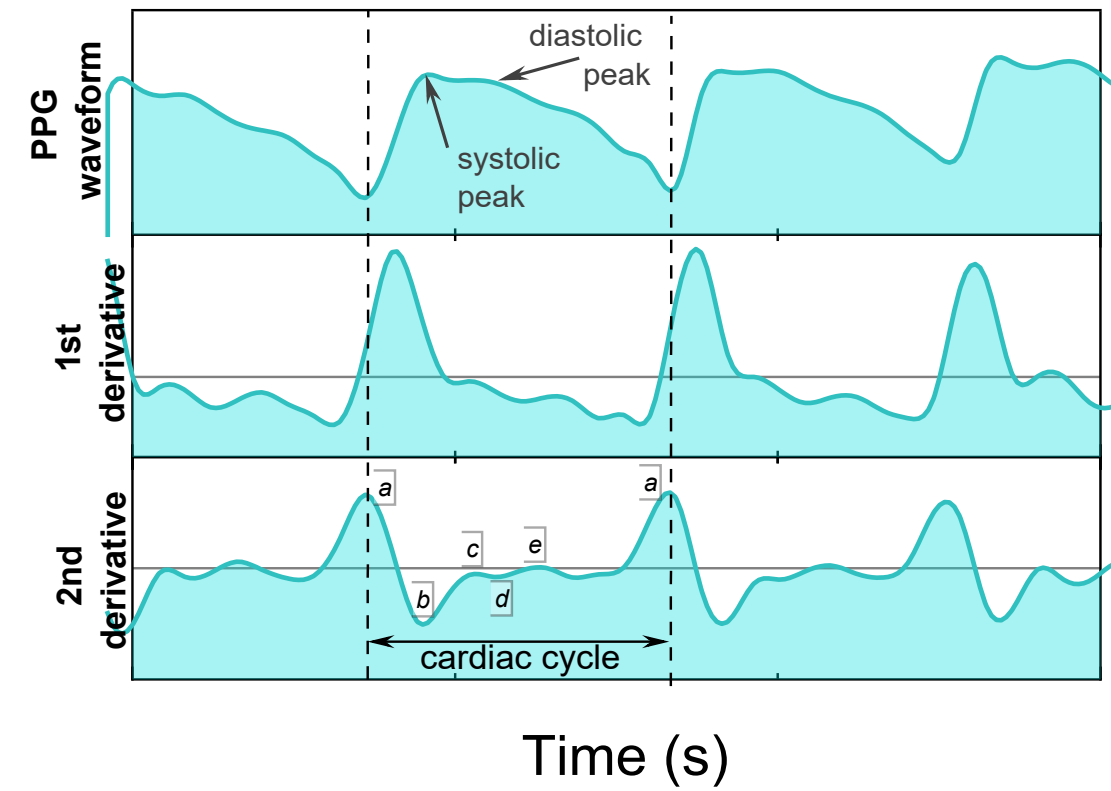
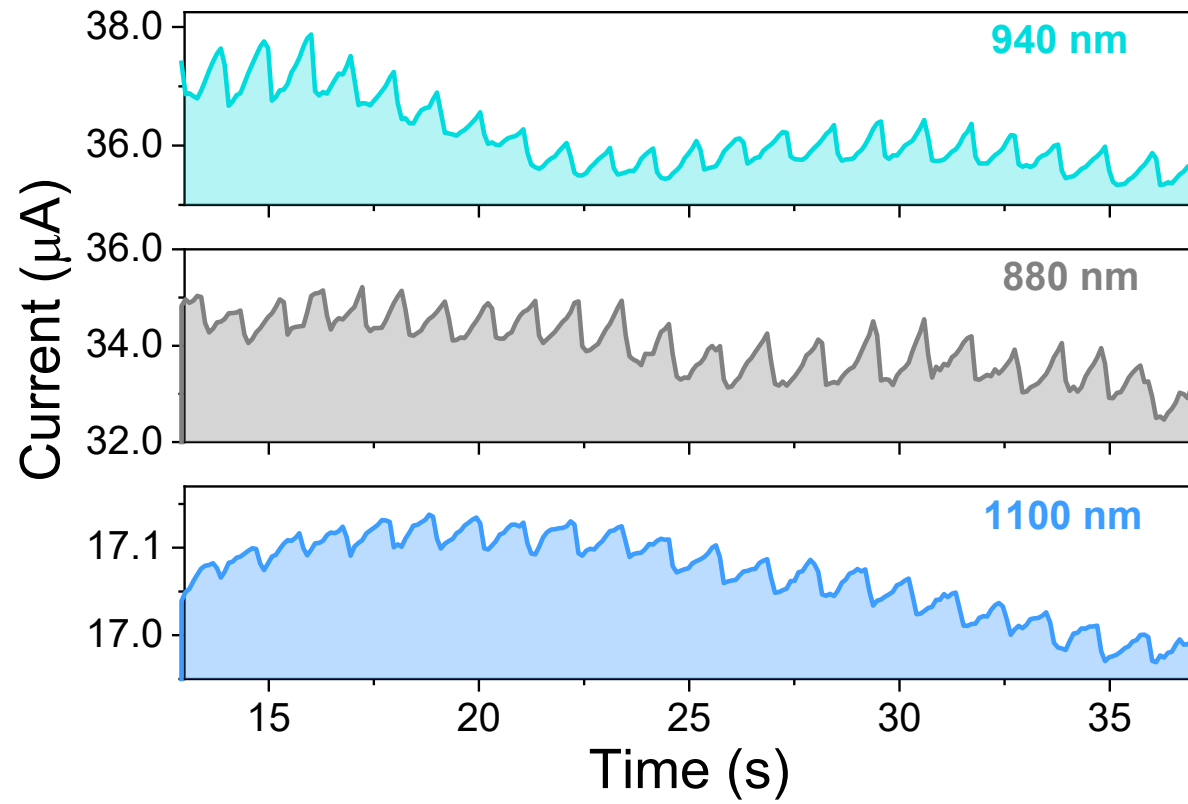


D^* of 10^{10} Jones 400-1350 nm!

Device performances



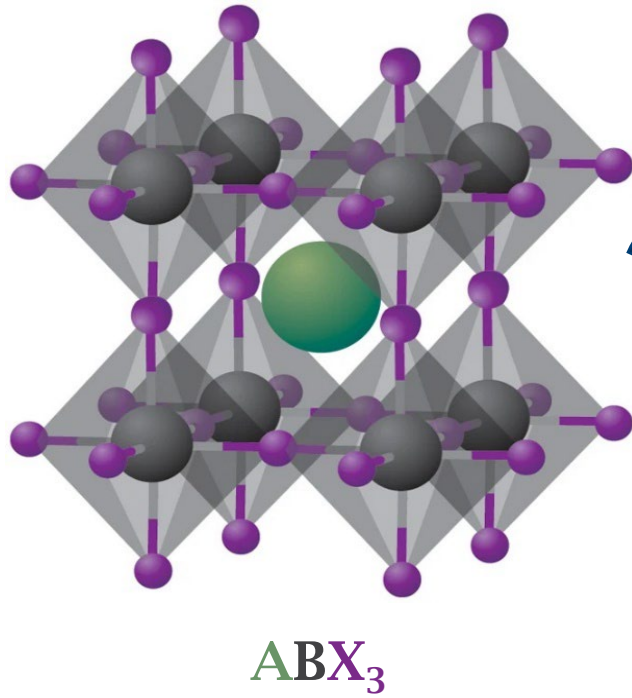
Real-world application



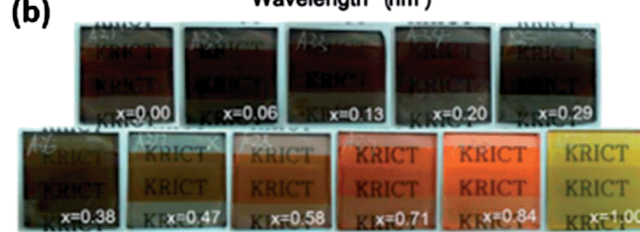
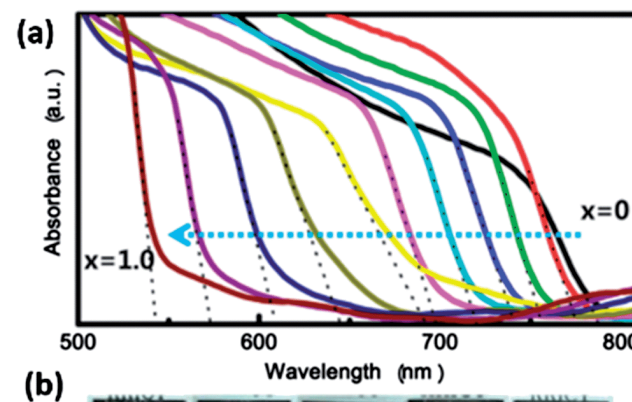
Perovskite Photodetectors

44

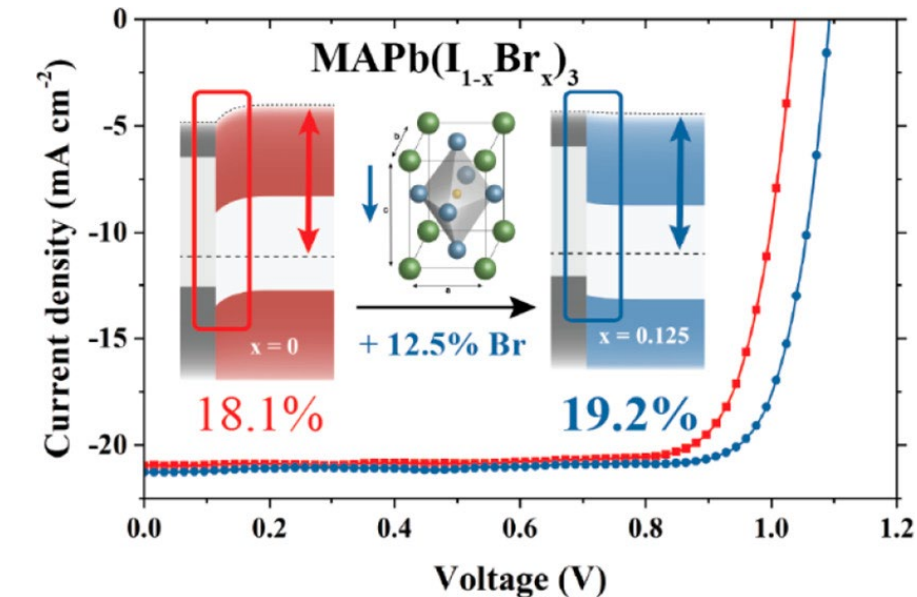
Imperial College London



A = monovalent organic cation
B = divalent metal cation
X = monovalent halogen anion



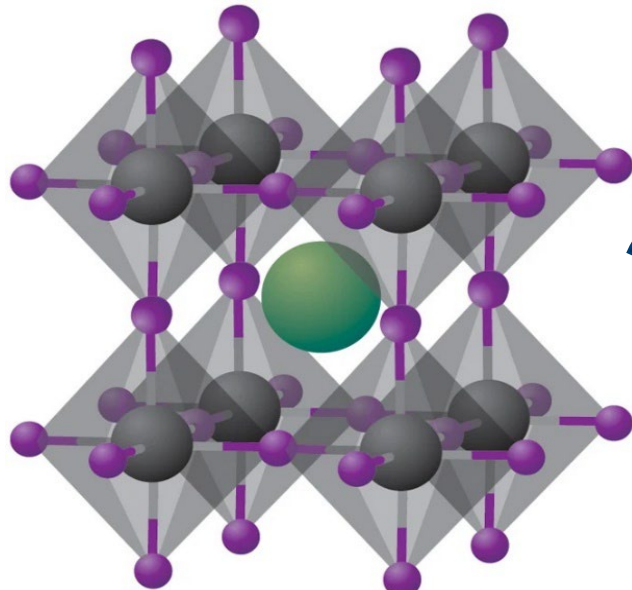
Tunable
bandgap
through
engineering



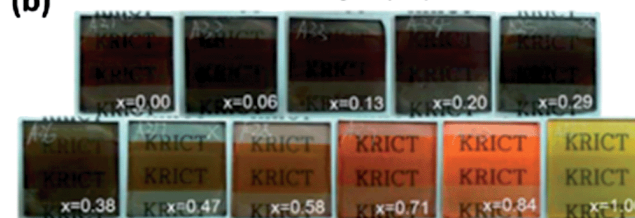
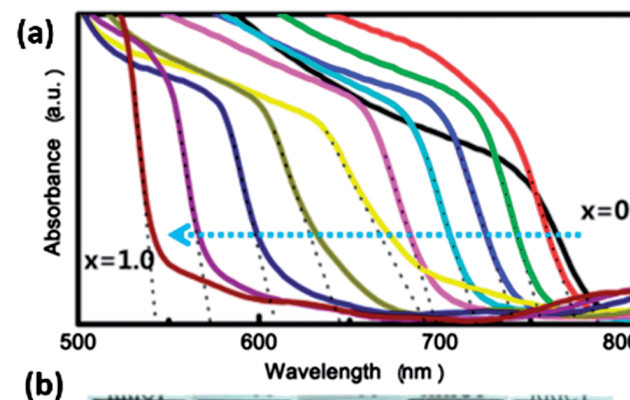
Perovskite Photodetectors

44

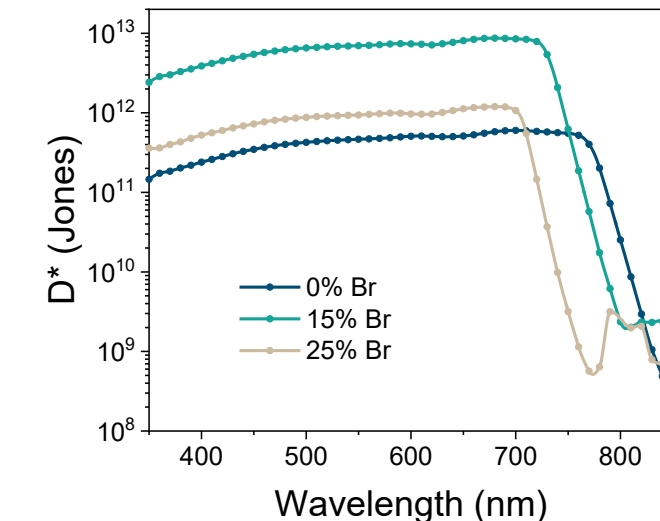
Imperial College
London



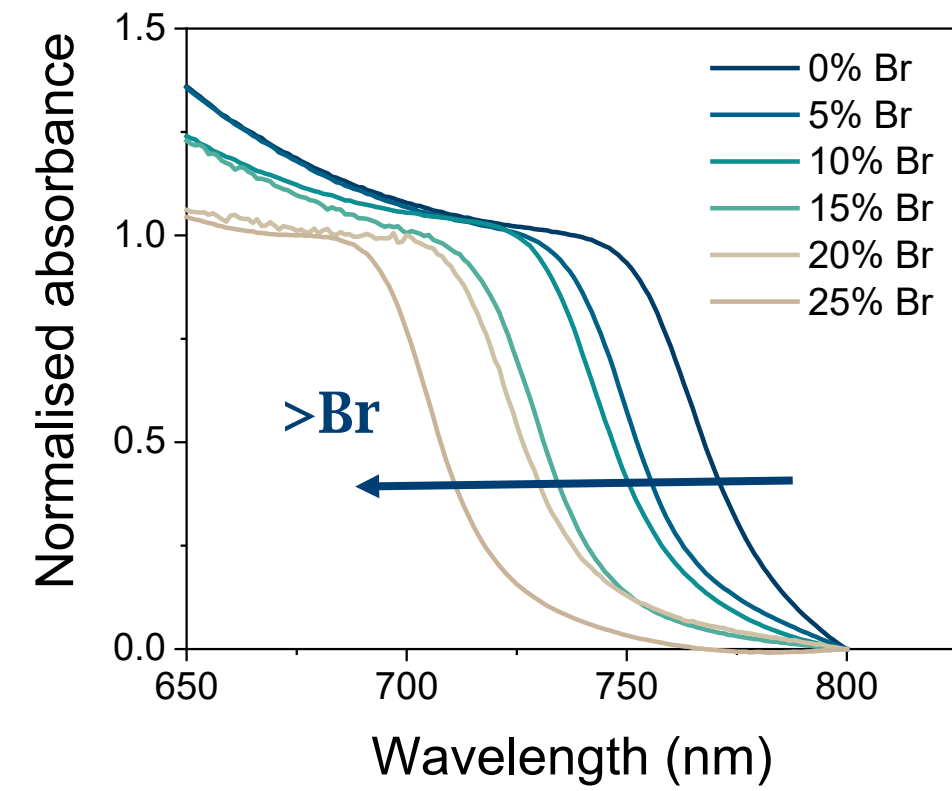
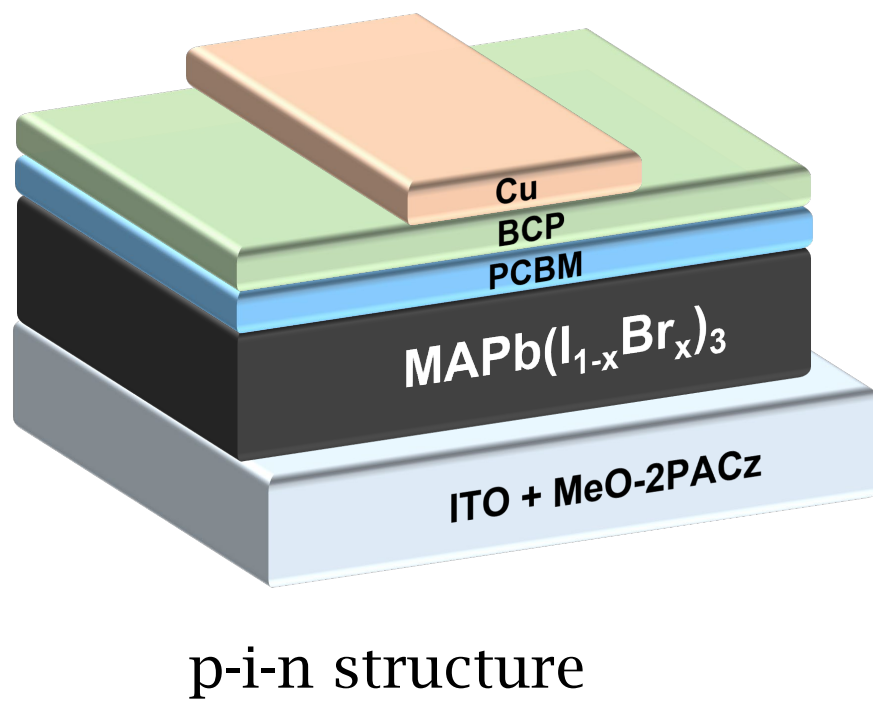
A = monovalent organic cation
B = divalent metal cation
X = monovalent halogen anion



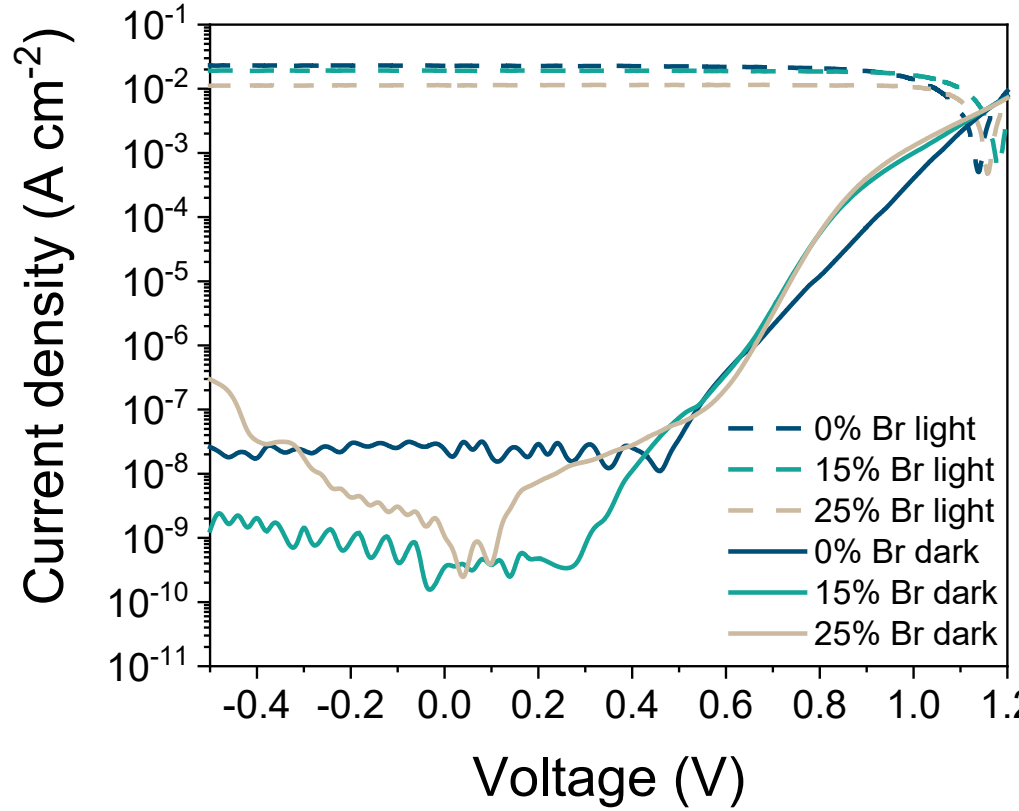
Tunable
bandgap
through
engineering



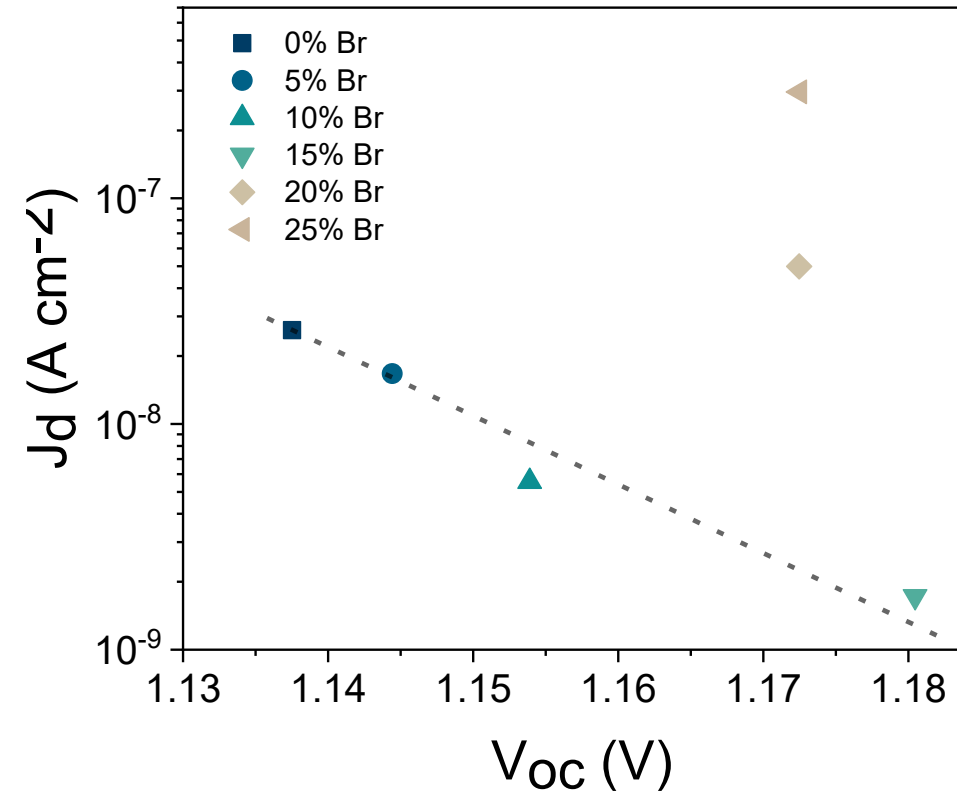
Reducing thermal charge generation: halide doping



Dark current



	$J_d (A\text{ cm}^{-2}) \text{ at } -0.5V$
0%Br	2.6×10^{-8}
15%Br	1.3×10^{-9}
25%Br	3.0×10^{-7}

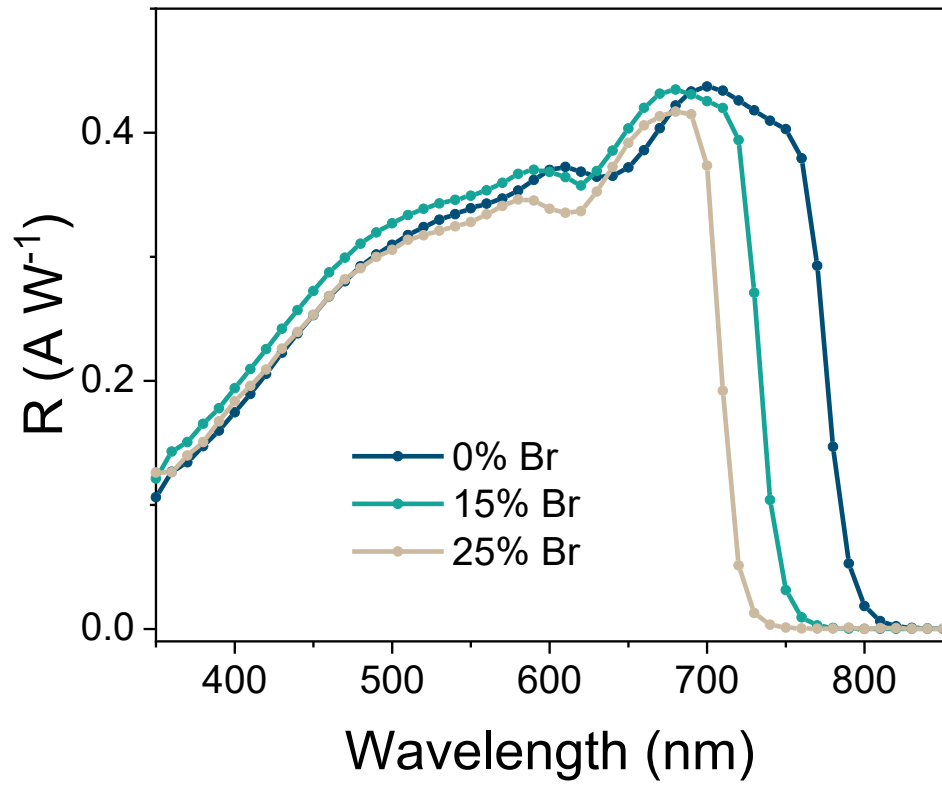


Exponential relationship between J_d and V_{oc} over the 0-15% Br range

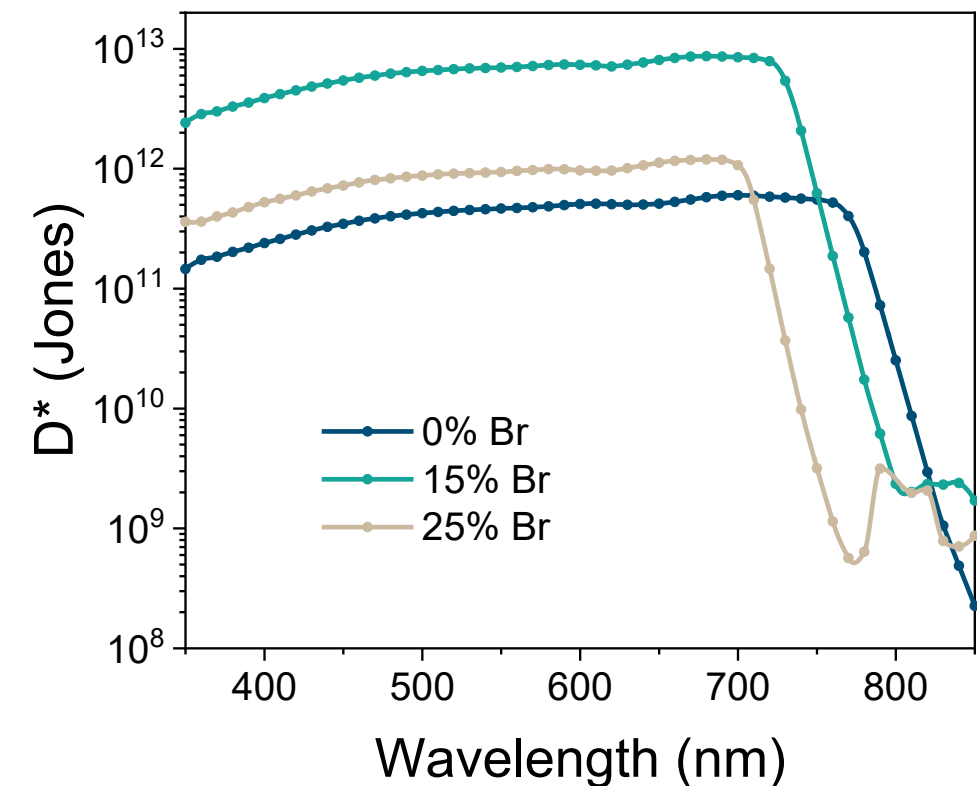
Similar behaviour as previously reported for organic PDs

Responsivity and Detectivity

$$SR(\lambda) = \frac{J_{ph}}{P_{in}} = EQE \cdot \frac{q\lambda}{hc} \quad [A \text{ } W^{-1}]$$



$$D^*(f, \lambda) = \frac{SR(\lambda)\sqrt{A\Delta f}}{i_{noise}(f)} \quad [Jones]$$



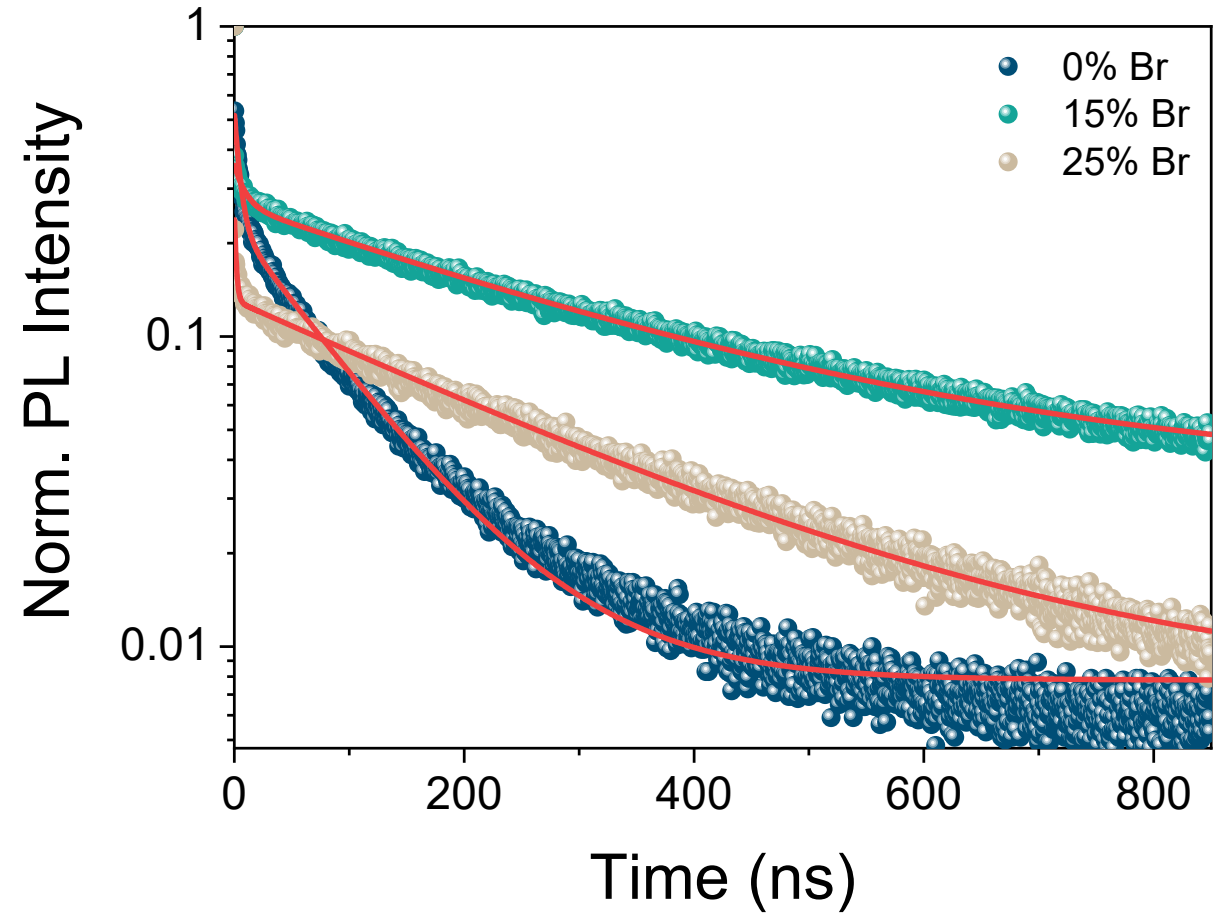
Recombination investigation

$$\tau_{ave,0\%}=80.28\text{ns}$$

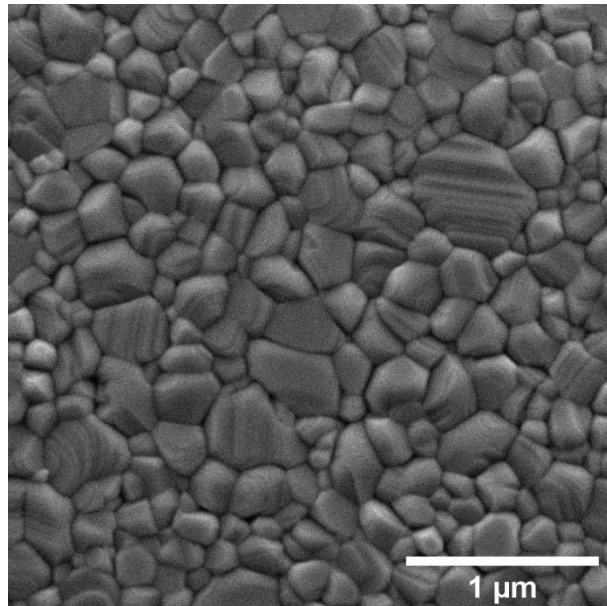
$$\tau_{ave,15\%}=299.31\text{ns}$$

$$\tau_{ave,25\%}=246.45\text{ns}$$

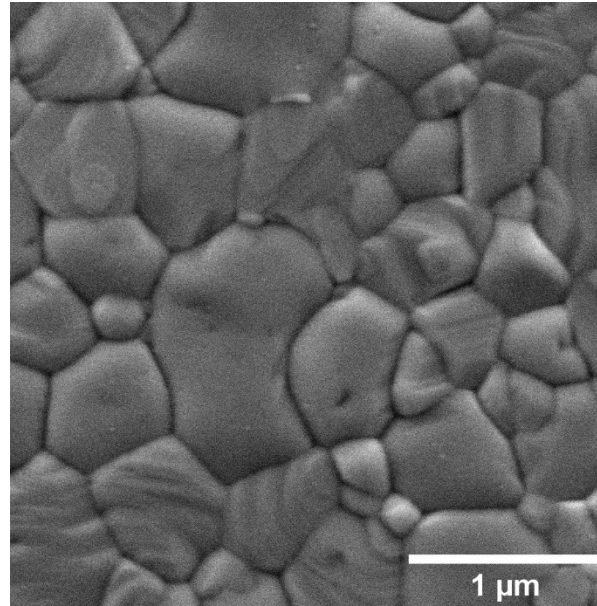
Long τ_{ave} represents suppressed non-radiative recombination pathways



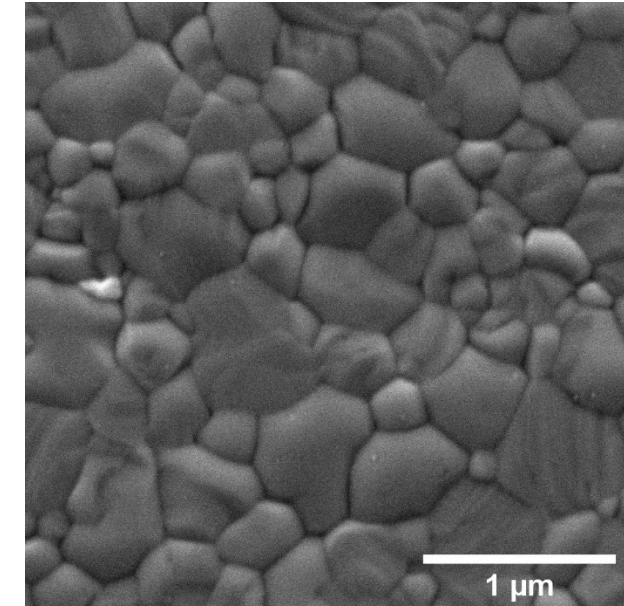
Morphological analysis



0% Br

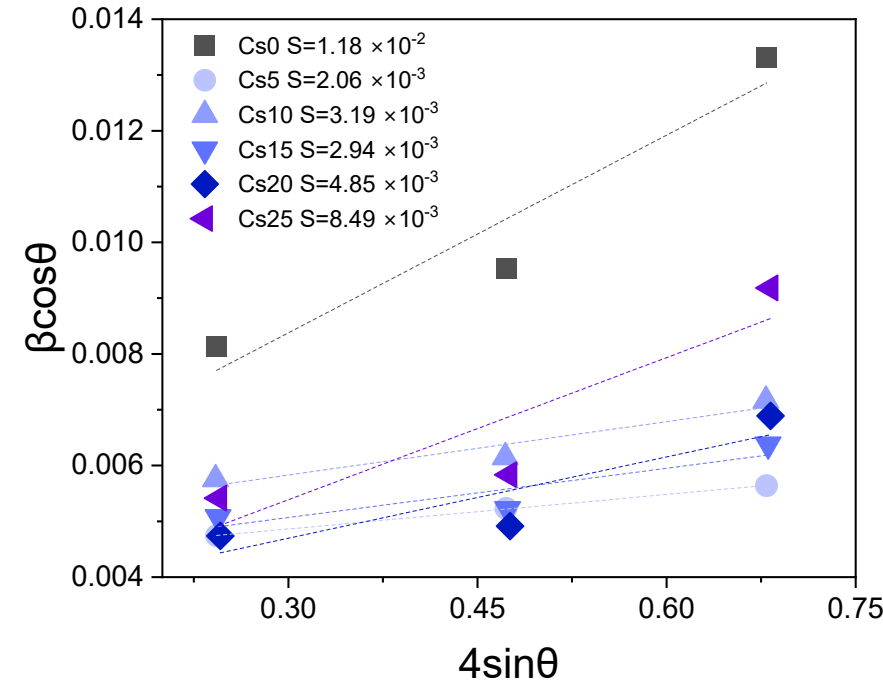
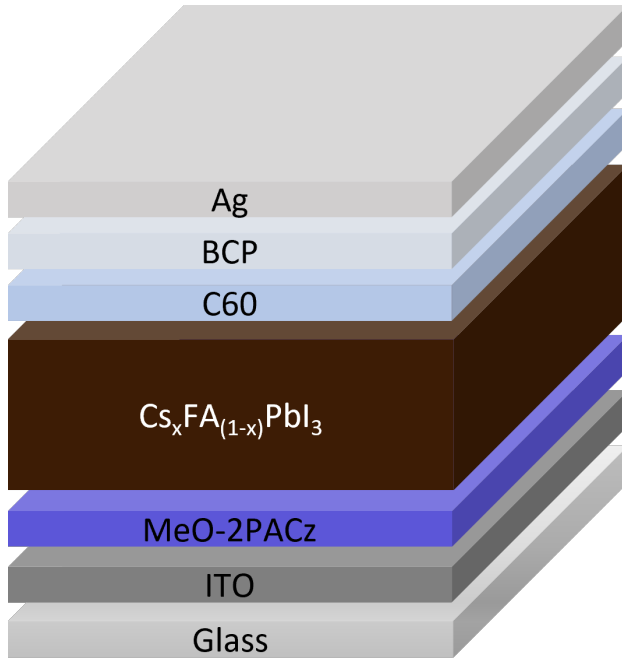


15% Br

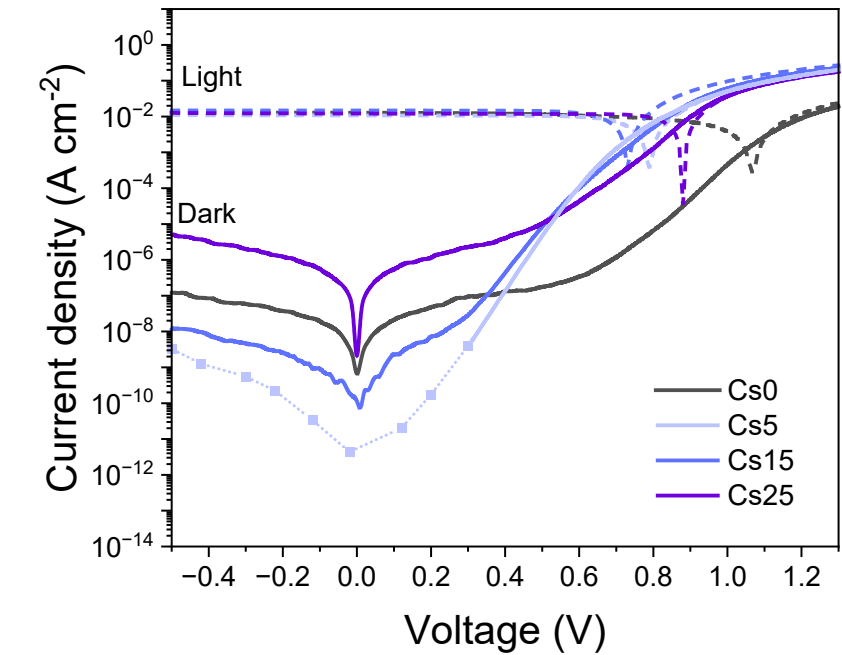


25% Br

Reducing J_d: Strain-induced α -phase stabilisation in FAPI-based Photodetectors

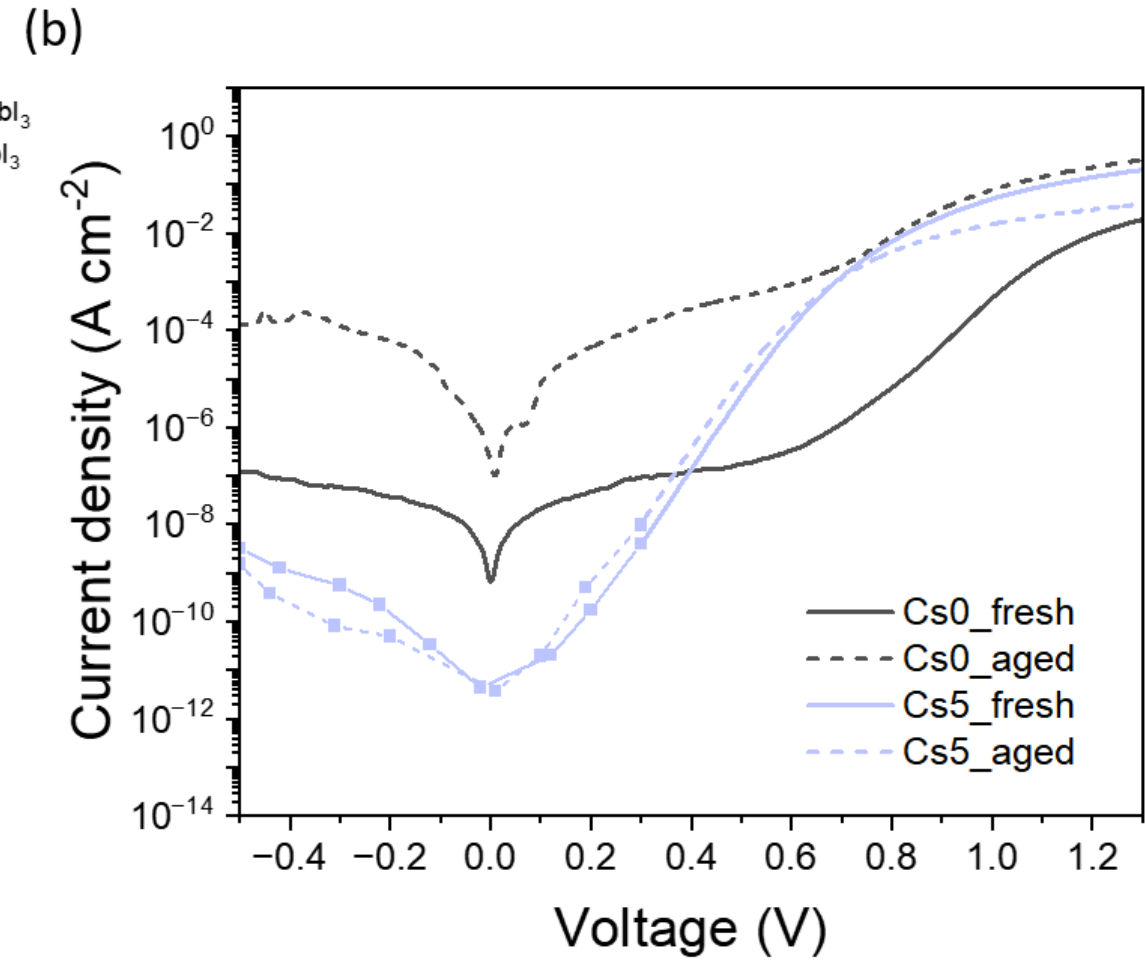
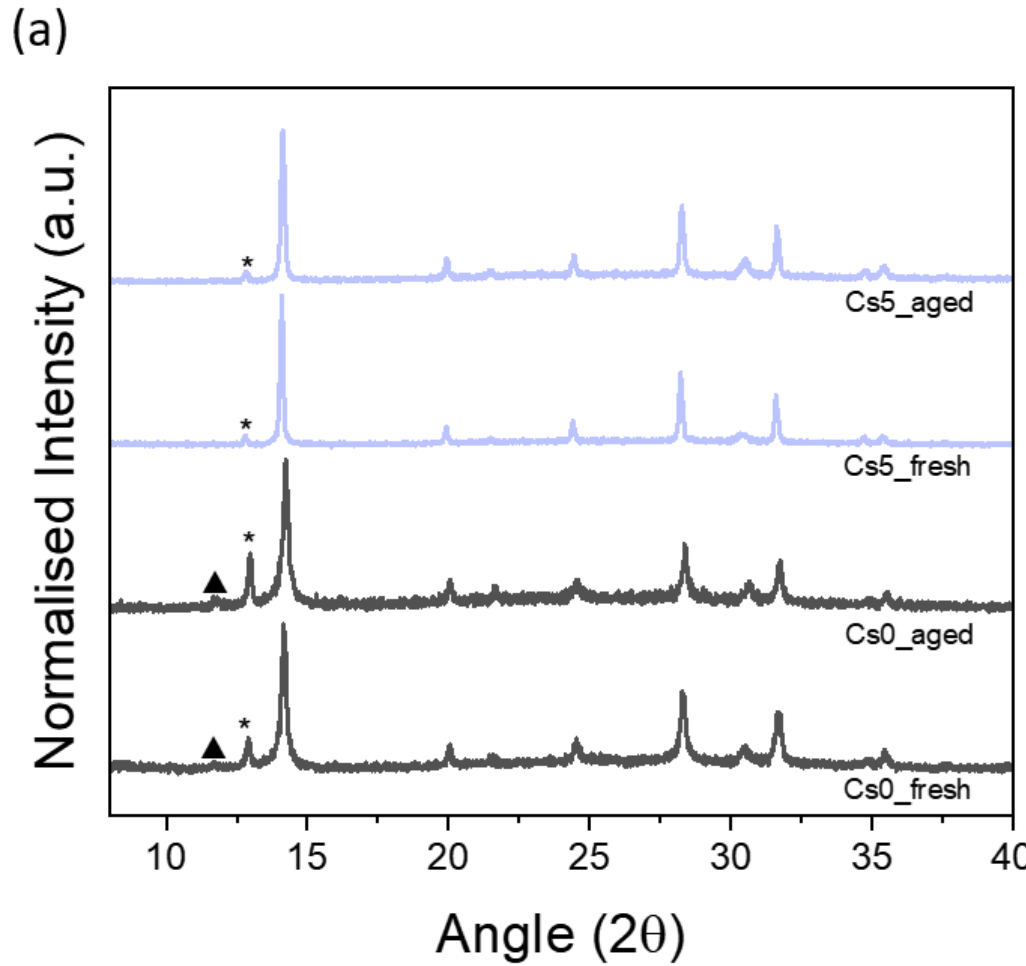


Cs5 → reduction in lattice strain

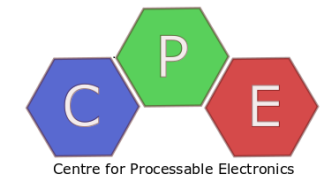


Cs5 → lowest J_d

α -phase stabilisation



Long-term stability of Cs5-based PD



Thank you for your attention

n.gasparini@imperial.ac.uk